2. Time and Reference Systems

Christopher Jekeli, Oliver Montenbruck

Geodesy is the science of the measurement and mapping of the Earth's surface, and in this context it is also the science that defines and realizes coordinates and associated coordinate systems. Geodesy thus is the foundation for all applications of global navigation satellite system (GNSS). This chapter presents the reference systems needed to describe coordinates of points on the Earth's surface or in near space and to relate coordinate systems among each other, as well as to some *absolute* system, visually, a celestial system. The topic is primarily one of geometry, but the geodynamics of the Earth as a rotating body in the solar system plays a fundamental role in defining and transforming coordinate systems. Therefore, also the fourth coordinate, time, is critical not only as the independent variable in the dynamical theories, but also as a parameter in modern geodetic measurement systems. Instead of expounding the theory of geodynamics and celestial mechanics, it is sufficient for the purpose of this chapter to describe the corresponding phenomena, textually, analytically and illustratively, in order to give a sense of the scope of the tasks involved in providing accurate coordinate reference systems not just to geodesists, but to all geoscientists.

2.1 **Time** 25
2.1.1 Dynamic Time 26
2.1.2 Atomic Time Scales 27
2.1.3 Sidereal and Universal Time, Earth Rotation 27
2.1.4 GNSS System Times 30

2.2 **Spatial Reference Systems** 31
2.2.1 Coordinate Systems 31
2.2.2 Reference Systems and Frames 34

2.3 **Terrestrial Reference System** 34
2.3.1 Traditional Geodetic Datums 34
2.3.2 Global Reference System 36
2.3.3 Terrestrial Reference Systems for GNSS Users 39
2.3.4 Frame Transformations 40
2.3.5 Earth Tides 42

2.4 **Celestial Reference System** 44

2.5 **Transformations Between ICRF and ITRF** 46
2.5.1 Orientation of the Earth in Space 46
2.5.2 New Conventions 50
2.5.3 Polar Motion 52
2.5.4 Transformations 54

2.6 **Perspectives** 55

References 56

2.1 Time

Everyone experiences time, but when pressed no one can explain exactly what it is. Mathematically it can be defined as a coordinate in a fourth dimension (as did Einstein), or more traditionally, it is the independent variable in our theories of motion. Indeed, the only reason that we perceive time is that things change. We have relatively easy access to *units* of time because many of the changes that we observe are periodic. If the changing phenomenon varies with uniform period, then the associated *time scale* is uniform. Clearly, a desirable property of a description and realization of time is that its scale should be uniform at least in the local frame. However, very few observed dynamical systems have rigorously uniform time units. In the past, Earth's rotation provided the most suitable and evident phenomenon to represent the time scale, with the unit being a (solar) day [2.1]. It has been recognized for a long time, however, that Earth's rotation is not uniform (it is varying at many different scales: daily, bi-weekly, monthly, etc., and even slowing down over geologic time [2.2, p. 607]). In addition to scale or units, an origin must be defined for a time system, that is, a zero-point, or an epoch, at which a value of time is specified. Finally, whatever system of time is defined, it should be accessible and, thereby, realizable, thus creating a time *frame*. This distinction between a system and a frame is explained in greater detail with respect to spatial coordinates in Sect. 2.2.2.

Prior to 1960, a second of time was defined as 1/86 400 of a mean solar day (Sect. 2.1.3). Today (since 1960), a fundamental time scale is defined by the natural oscillation of the cesium atom and all time systems can be referred or transformed to this scale. Specifically, the SI (*Système International*) second is defined as follows [2.3, 4]:

> *The second is the duration of* 9 192 631 770 *periods of the radiation corresponding to the transition between the two hyperfine levels of the ground state of the cesium* 133 *atom.*

This definition has been refined to specify that the atom should be at rest (i. e., at temperature 0 K) and at mean sea level, thus independent of ambient radiation effects and relativistic gravitational changes. Corrections are applied to actual measurements to comply with these requirements. The value of the SI second was set to the previously (in 1956) adopted value of a second of *ephemeris time* (ET) (Sect. 2.1.1), defined as 1/31 556 925.9747 of a mean tropical (solar) year, being computed for the epoch, 1 January 1900, on the basis of Newcomb's theory of motion of the Earth around the Sun [2.5].

Although the SI second now defines the fundamental time unit, one still distinguishes between systems of time that have different origins and even different scales depending on the application. Dynamic time is the independent variable in the most complete theory of the dynamics of the solar system. It is uniform by definition. Mean solar time, or universal time (UT), is the time scale based on Earth's rotation with respect to the Sun and is used for general civilian time keeping. Finally, sidereal time is defined by Earth's rotation with respect to the celestial sphere. Within this section, the various types of dynamic, atomic, and sidereal time scales are described in further detail.

2.1.1 Dynamic Time

Newtonian (ephemeris time) and relativistic (barycentric and terrestrial time (TT), etc.) concepts of *dynamic time* generally refer to the time variable in the equations of motion describing the dynamical behavior of the massive bodies of our solar system. As such, with respect to the theory of general relativity, the dynamic time scale refers to a coordinate system and thus represent a coordinate time (Chap. 5). Common choices include the *barycentric* reference system (origin at the center of mass of the solar system) or the *geocentric* reference system. The corresponding time scales are thus designated as *barycentric coordinate time* (TCB) and *geocentric coordinate time* (TCG). Note that acronyms for time systems generally follow the corresponding French names, for example, *temps-coordonnée barycentrique* for Barycentric Coordinate Time. Dynamic time defined in this way is the fourth coordinate and transforms according to the theory of general relativity as the fourth coordinate from one point in space–time to another.

On the other hand, dynamic time has also been defined as a *proper time*, the time associated with the frame of the observer that a uniformly running clock would keep and that describes observed motions in that frame. Depending on the frame of the observer, it is designated, for example, *terrestrial dynamic time* (TDT), or *barycentric dynamic time* (TDB). In 1991, the International Astronomical Union (IAU) renamed TDT simply *terrestrial time*, referring to proper time at the geoid (approximately mean sea level). However, in 2000 the IAU further recommended, due to uncertainties in the realization of the geoid, that TT be redefined as differing from TCG by a constant, specified rate. Its relation to a proper time then more precisely depends on the location and velocity of the observer's clock in the ambient gravitational field. Mathematical connections to the coordinate times, TCB and TCG, and to TDB may be found in Chap. 5 of this Handbook as well as in [2.6, Chap. 10]. The realization of TT is atomic time (Sect. 2.1.2), that is, its scale is the SI second. For calculations of Earth orientation (Sect. 2.5.1), the difference between TT and TDB is usually neglected.

Prior to 1977, the dynamic time was called *ephemeris time*. ET was based on the time variable in the theory of motion of the Sun relative to the Earth – Newcomb's ephemeris of the Sun. This theory suffered from the omission of relativistic theory, the dependence on adopted astronomical constants that, in fact, show a time dependency (such as the *constant* of aberration). It also omitted the effects of other planets on Earth's orbit. The new dynamic time described above was constrained to be consistent with ET at their boundary; specifically,

$$\mathrm{TT} = \mathrm{ET} \ \text{ at } \ 1977 \ \text{ January } \ 1.0003725 \\ \left(1^{\mathrm{d}}\ 0^{\mathrm{h}}\ 00^{\mathrm{m}}\ 32.184^{\mathrm{s}},\ \text{exactly}\right). \tag{2.1}$$

The extra fraction in this epoch was included since this would make the point of continuity between the systems exactly January 1.0, 1977, in International Atomic Time (TAI) (Sect. 2.1.2).

The basic unit of dynamic time is the *Julian Day*, equal to 86 400 SI seconds, which is close to our usual day based on Earth rotation, but is uniform by definition. The origin of dynamic time, designated by the *Julian date*, or *Julian epoch*, J0.0, is defined to be Greenwich noon, 1 January 4713 BC. Julian days, by convention, start and end when it is noon (dynamic

time) in Greenwich, England, representing midday in the usual meaning of a day starting and ending at midnight. Furthermore, there are exactly 365.25 Julian days in a *Julian year*, or exactly 36 525 Julian days in a *Julian century*. With the origin as given above, the Julian date, J1900.0, corresponds to the Julian day number, 2 415 021.0, being Greenwich noon, January 1, 1900; and the Julian date, J2000.0, corresponds to the Julian day (JD) number 2 451 545.0, being Greenwich noon, January 1, 2000 (Fig. 2.1). Thus, the date with Julian day number 2 451 545.0 is also January 1.5, 2000. Note that January 0.5, 2000 is really Greenwich noon on December 31, 1999 (or December 31.5, 1999). For practical reasons, a *modified* Julian day number

$$\mathrm{MJD} = \mathrm{JD} - 2\,400\,000.5\,, \tag{2.2}$$

is also defined relative to a new origin, which counts days as starting at midnight in Greenwich.

2.1.2 Atomic Time Scales

Atomic time refers to the time scale defined and realized by the oscillations in energy states of the cesium-133 atom, as defined in the introduction of this section. The SI second thus is the unit that defines the atomic time scale [2.3, 7]. Atomic time was not realized until 1955 with the development of standardized atomic clocks (Chap. 5). From 1958 through 1968, the *Bureau International de l'Heure* (BIH) in Paris maintained the atomic time scale. The origin, or zero point, for atomic time has been chosen officially as $0^h\,0^m\,0^s$, January 1, 1958.

International Atomic Time was officially introduced in January 1972. It was determined and subsequently defined that on $0^h\,0^m\,0^s$, January 1, 1977 (TAI), the ET epoch was $0^h\,0^m\,32.184^s$, January 1, 1977 (ET); thus, in accord with (2.1),

$$\mathrm{TAI} = \mathrm{TT} - 32.184\,\mathrm{s}\,. \tag{2.3}$$

TAI is realized today by the *Bureau International des Poids et Mesures* (BIPM), which combines data from over 400 high-precision atomic clocks around the world in order to maintain the SI-second scale as accurately as possible. TAI is published and accessible as a correction to each time-center clock, but rather in terms of *coordinated universal time* (UTC, Sect. 2.1.3), which is civilian atomic time adjusted to be close to a time scale based on Earth's rotation.

In the United States, the official atomic time clocks are maintained by the US Naval Observatory (USNO) in Washington, DC, and by the National Institute of Standards and Technology (NIST) in Boulder, CO, USA. Within each such center several cesium beam clocks are running simultaneously and averaged. Other centers participating in the realization of TAI include observatories in Paris, Greenwich, Moscow, Tokyo, Ottawa, Wettzell, Beijing, and Sydney, among over 70 others. The comparison and amalgamation of the clocks of participating centers around the world are accomplished by LORAN-C, satellite transfers (GNSS playing the major role; Chap. 41), and actual clock visits. Time offsets of individual laboratories and their uncertainties are reported in the monthly issues of the BIPM Circular T [2.8]. Worldwide synchronization for many of the national laboratories is at the level of a few tens of nanoseconds or better [2.9]. Since atomic time is computed from many clocks, it is also known as a *paper clock* or a *statistical clock*.

2.1.3 Sidereal and Universal Time, Earth Rotation

Sidereal time represents the rotation of the Earth with respect to the celestial sphere and reflects the actual rotation rate of the Earth, plus effects due to the small motion of the spin axis relative to space (precession and nutation, Sect. 2.5.1). It is the angle on the equator between a particular terrestrial meridian and the *vernal equinox*, ♈, which is the point on the celestial sphere where the Sun crosses the equator in Spring

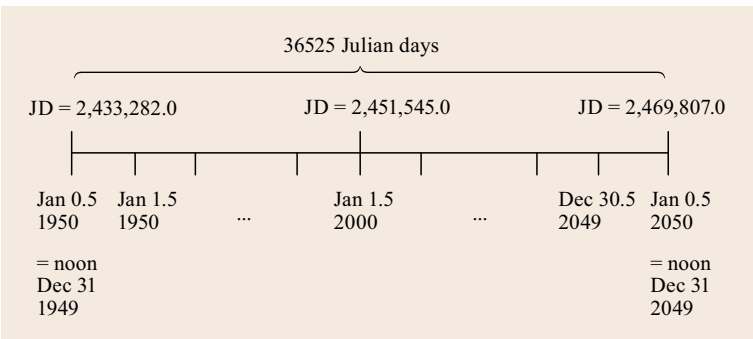

Fig. 2.1 Julian Day numbers and their relation to our current conventional calendar

as viewed by the Northern Hemisphere of the Earth. Inasmuch as the equator has the same dynamics as the spin axis, one distinguishes between apparent (or, true) and mean sidereal time, the latter having the effects of nutation removed. The amplitude of this effect is about 15.8″, which corresponds to about 1 s of time using the conversion, 15° = 1 h. *Greenwich apparent sidereal time* (GAST) is the angle from the true (or, instantaneous) equinox to the Greenwich meridian (Fig. 2.2).

Due to the precession of the spin axis and thus the vernal equinox on the equator, sidereal time includes a small rotation rate (about $7.1 \cdot 10^{-12}$ rad/s) that is not due to Earth rotation. For this reason, a new origin point, σ, has been introduced and adopted in the late 1990s that better serves the determination of Earth's rotation rate. This so-called nonrotating origin is also called the celestial intermediate origin (CIO) as explained in Sect. 2.5.2. A new angle, θ, called the Earth rotation angle (ERA), now represents true Earth rotation (Fig. 2.2). The angle $\alpha(\Upsilon) = \theta - \text{GAST}$, also called the equation of origins (EO), today (2015) has a significant value of about −12′ due to the accumulated precession since J2000. Expressions for evaluating the EO at arbitrary epochs are provided in [2.6, 10].

UT is the time scale used for general civilian time keeping and is based approximately on the diurnal motion of the Sun. However, the Sun, as viewed by a terrestrial observer does not move uniformly on the celestial sphere. To create a uniform time scale requires the notion of a fictitious, or *mean Sun*, and the corresponding time is known as *mean solar time* (MT). UT is defined as mean solar time on the Greenwich meridian. The basic unit of UT is the *mean solar day*, being the time interval between two consecutive transits of the mean Sun across the meridian. The mean solar day has 24 mean solar hours and 86 400 mean solar seconds.

In comparison to sidereal time, the following approximate relations hold

$$\begin{aligned}&1 \text{ mean solar day}\\&= 24^{\text{h}}\,03^{\text{m}}\,56.5554^{\text{s}} \text{ in sidereal time}\,,\end{aligned} \tag{2.4}$$

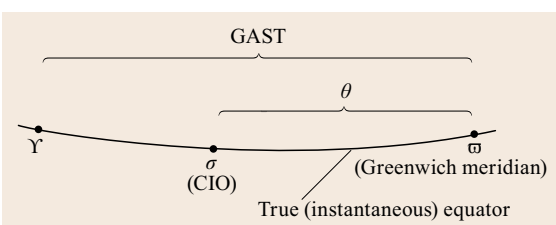

Fig. 2.2 Relationship between GAST and the Earth rotation angle, θ, relative to the true vernal equinox, ϒ

$$\begin{aligned}&1 \text{ mean sidereal day}\\&= 23^{\text{h}}\,56^{\text{m}}\,04.0905^{\text{s}} \text{ in solar time}\,.\end{aligned} \tag{2.5}$$

A mean solar day is longer than a sidereal day because in order for the Sun to return to the observer's meridian, the Earth must rotate an additional amount due to its orbital advance (Fig. 2.3). Thus, also Earth's rotation rate is *not* equal to $2\pi/86\,400$ rad/s if s is a solar second. Instead, the rate is, according to (2.5),

$$\omega_{\oplus} = 7.292115 \cdot 10^{-5} \text{ rad/s}\,. \tag{2.6}$$

To determine $\omega_{\oplus}$ (and its variations) from measurements by terrestrial observers, one must account for the fact that the observer's reference meridian is associated with a fixed pole, with respect to which the Earth's spin axis moves (polar motion, Sect. 2.5.3). In addition, Earth's rotation is affected by other irregularities of periodic and secular character (such as seasonal effects and the exchange of angular momentum between the Earth and Moon) that are lumped into so-called *length-of-day variations*. Universal time as a scale derived from Earth's rotation has thus been separated into:

UT0: Universal Time determined from observations with respect to the meridian fixed to the reference pole;
UT1: Universal Time determined with respect to the meridian attached to the spin axis;
UT2: Universal Time UT1 corrected for seasonal variations.

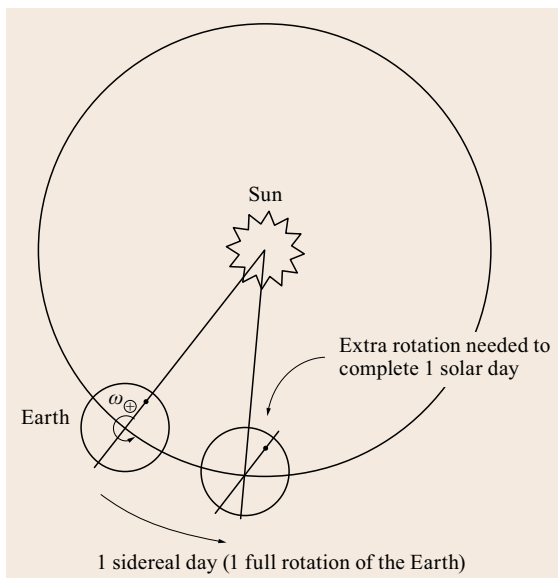

Fig. 2.3 Geometry of sidereal and solar days

UT2 is the best approximation of UT to a uniform time, although it is still affected by small secular variations. However, as a matter of practical utilization it has now been replaced by an atomic time scale (UTC, see below).

In terms of the SI second, the mean solar day is given by

$$1^{\mathrm{d}}\,(\mathrm{MT}) = 86\,400\,\mathrm{s} - \frac{\Delta\tau}{n}\,, \tag{2.7}$$

where

$$\Delta\tau = \mathrm{UT1} - \mathrm{TT} \tag{2.8}$$

is the difference over a period of n days between UT1 and dynamic time. The length-of-day variation is the time-derivative of $\Delta\tau$. From observational records over the centuries it has been found that the secular variation in the length of a day (rate of Earth rotation) currently is approximately +1.4 ms per century [2.2, p. 607].

All civilian clocks in the world are now set with respect to an atomic time standard since atomic time is much more uniform than solar time and more easily realized through time transfer by satellite signals. Yet, there is still a desire (particularly, in the astronomic community) that civil time should correspond to solar time; therefore, a new atomic time was defined that approximates UT. This atomic time is called *Coordinated Universal Time* (UTC) and implemented in accord with Recommendation TF.460 of the International Telecommunication Union (ITU) [2.11]:

> *UTC is the time scale maintained by the BIPM, with assistance from the IERS, which forms the basis of a coordinated dissemination of standard frequencies and time signals. It corresponds exactly in rate with TAI but differs from it by an integral number of seconds. The UTC scale is adjusted by the insertion or deletion of seconds (positive or negative leap seconds) to ensure approximate agreement with UT1.*

Initially, UTC was adjusted so that $|\mathrm{UT2} - \mathrm{UTC}| < 0.1\,\mathrm{s}$. As of 1972, the requirement for the correspondence between UTC and UT was relaxed to

$$|\mathrm{UT1} - \mathrm{UTC}| < 0.9\,\mathrm{s}\,. \tag{2.9}$$

The adjustments, called *leap seconds*, are introduced either January 1 or July 1 of any particular year.

Up to 2015, leap seconds have, on average, been introduced approximately once every 1.5 years (Table 2.1). Following an earlier adjustment in July 2012, the UTC – TAI amounts to −36 s since mid 2015. The history of UTC relative to TAI and other time scales is schematically shown in Fig. 2.4 based on tabulated data of the United Sates Naval Observatory (USNO) in [2.12]. The decision to introduce new leap seconds is taken by the *International Earth Rotation and Reference Systems Service* (IERS) and announced within the IERS Bulletin C.

Table 2.1 UTC leap seconds introduced since 1972. The table provides the integer seconds difference between UTC and TAI along with the starting date of applicability (after [2.12])

Since	UTC – TAI (s)	Since	UTC – TAI (s)
1 Jan 1972	−10	1 Jan 1988	−24
1 Jul 1972	−11	1 Jan 1990	−25
1 Jan 1973	−12	1 Jan 1991	−26
1 Jan 1974	−13	1 Jul 1992	−27
1 Jan 1975	−14	1 Jul 1993	−28
1 Jan 1976	−15	1 Jul 1994	−29
1 Jan 1977	−16	1 Jan 1996	−30
1 Jan 1978	−17	1 Jul 1997	−31
1 Jan 1979	−18	1 Jan 1999	−32
1 Jan 1980	−19	1 Jan 2006	−33
1 Jul 1981	−20	1 Jan 2009	−34
1 Jul 1982	−21	1 Jul 2012	−35
1 Jul 1983	−22	1 Jul 2015	−36
1 Jul 1985	−23	1 Jan 2017	−37

The lengthening of a day by about 1.4 ms per century as measured by Earth's slowing rate of rotation implies that the UT1 clock continues to run more and more behind the TAI clock. It has been determined that the mean solar day today is actually about 86 400.0027 SI seconds long, since the SI second was originally identified with the ET second based on the motion of the mean Sun at Newcomb's time in the nineteenth century. Indeed, 86 400 SI seconds exactly equaled a mean solar day in 1820, or 1.95 centuries (cy) ago. This disparity between the scales of the defined SI second and the current mean solar day has an accumulative effect that adds, on the average, about $1.4\,\mathrm{ms/d/cy} \times 1.95\,\mathrm{cy}$, or about 1 s to UT1 during the course of a year; hence, the introduction of the leap seconds. The difference, $\mathrm{DUT1} = \mathrm{UT1} - \mathrm{UTC}$, is broadcast along with UTC so that users can determine UT1.

The relationships among the various atomic time scales are illustrated along with dynamic time in Fig. 2.4. There is current debate [2.13–15] about the need to maintain the small difference between UTC and UT1 considering the technical inconveniences and inefficiencies (if not outright difficulties) this imposes on the many modern civilian telecommunications systems and other networks that rely on a precise time scale.

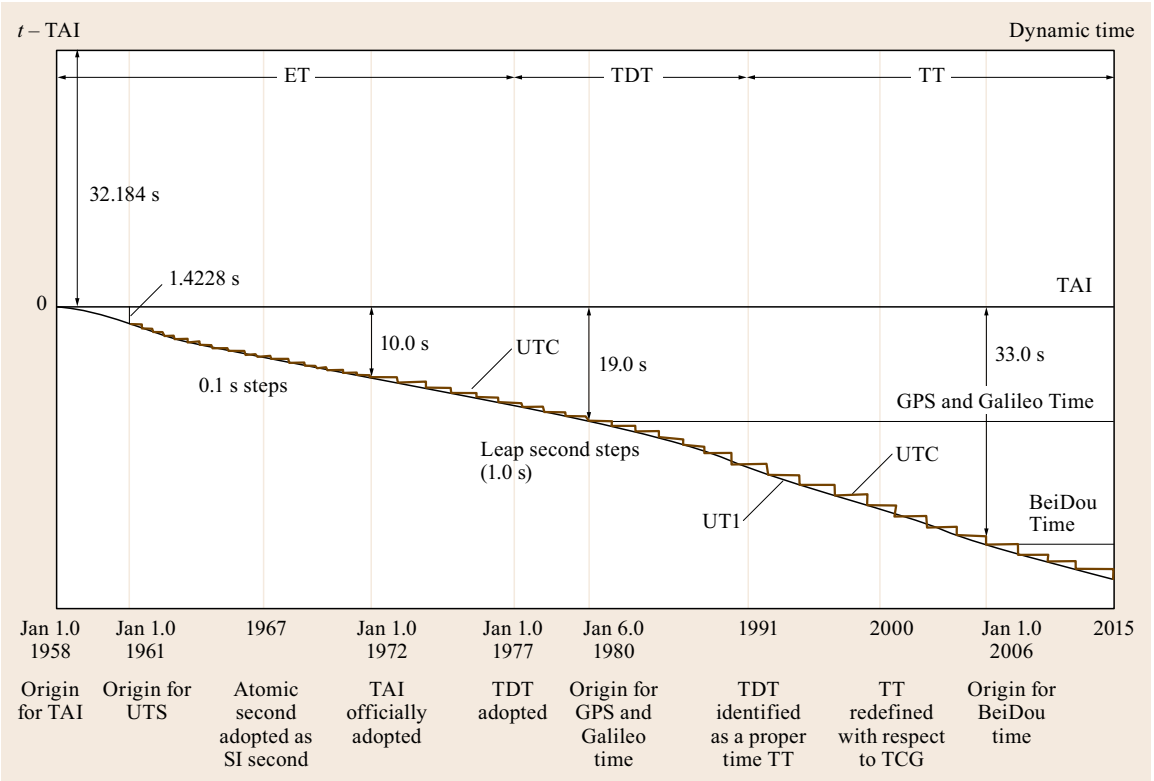

Fig. 2.4 Relationships between atomic time scales and dynamic time (indicated leap seconds are schematic only). For the acronyms, see the text

2.1.4 GNSS System Times

Satellite navigation systems provide user coordinates derived from distance measurements that are based on the propagation time of the transmitted signals. Thus, all these systems rely on very accurate clocks and time standards. To meet the needs of internal time synchronization and dissemination, each GNSS maintains a specific *system time*. The time systems of the four global navigation satellite systems, Global Positioning System (GPS), GLONASS, Galileo, and BeiDou, are all based on the SI second and atomic time similar to TAI. However, they are realized by different clock ensembles and have different origins and offsets with respect to TAI [2.16].

GPS time (GPST) is the system time employed by the United States' Global Positioning System. Since 1990, it is formed as a *composite clock* from atomic clocks within the GPS Control Segment (including both the Master Control Station and the Monitoring Stations) as well as the atomic frequency standards onboard the GPS satellites [2.17, 18]. Each of these clocks contributes to the resulting time scale with a specific weight based on the observed variance of the respective clock [2.19]. Using common view time transfer, GPS time is steered to deviate by at most 1 µs [2.20] from UTC(USNO), that is, the realization of UTC maintained by the United States Naval Observatory. In practice, the GPS – UTC(USNO) offset is much smaller than the specified range and achieves representative values at the level of 20 ns [2.21]. In order to provide GPS users with access to UTC, a forecast value of the offset between both time scales is transmitted as part of the navigation message.

The origin of GPS time, as noted in Fig. 2.4, is January 6.0, 1980 UTC(USNO). However, GPS time is not adjusted by leap seconds to slow down with UT and it is thus permanently offset (late) by a constant amount from TAI

$$t\,(\mathrm{GPS}) = \mathrm{TAI} - 19\,\mathrm{s}\,. \tag{2.10}$$

At the same time, it is offset from (ahead of) UTC by varying amounts depending on the number of introduced leap seconds. Note that (2.10) describes only the nominal (integer second) offset between GPS time and

TAI, but neglects additional fractional offsets (typically at the level of tens of nanoseconds) related to different realization of the two time scales.

GLONASS Time (GLST) is the only GNSS time scale that actually follows the ITU recommendation [2.11] to align a disseminated time scale with UTC. Its origin is chosen as January 1.0, 1996 in the UTC(SU) time system, that is, the Russian (formerly Soviet Union, SU) realization of UTC maintained by the Institute of Metrology for Time and Space in Moscow. Besides incorporating leap seconds, GLST is always 3 h ahead of UTC because of the time zone difference between Greenwich and Moscow. Thus,

$$t\,(\mathrm{GLONASS}) = \mathrm{UTC} + 3\,\mathrm{h}\,. \tag{2.11}$$

Again, this relation does not account for fractional second offsets resulting from the independent realization of both time scales. GLST is obtained from an ensemble of hydrogen-masers in the GLONASS ground segment and synchronized to UTC(SU) using two-way time transfer with a specified tolerance of 1 µs [2.22]. Following a consolidated effort to improve the alignment of GLST with UTC, the difference of the two time scales has improved from several hundred ns [2.23] to a few tens of ns as of the second half 2014 [2.24].

Both the *Galileo System Time* (GST, [2.25, 26]) and *BeiDou time* (BDT; [2.27]) exhibit a constant offset from TAI. The origin for Galileo time, for consistency, is defined to be identical to that of GPS Time, but the origin for the BeiDou time system has been chosen as January 1.0, 2006 UTC. Thus,

$$t\,(\mathrm{Galileo}) = \mathrm{TAI} - 19\,\mathrm{s}\,, \tag{2.12}$$

$$t\,(\mathrm{BeiDou}) = \mathrm{TAI} - 33\,\mathrm{s}\,. \tag{2.13}$$

Both time scales are generated from atomic clocks in the respective control segments and steered to UTC via time transfer and clock comparison with other UTC laboratories. GST is specified to differ by less than 50 ns (2σ) from UTC [2.25, 28] while a maximum offset of 100 ns applies for BeiDou [2.23, 29].

Similar to Galileo, continuous time scales with a fixed −19 s offset from TAI are also adopted by the Japanese Quasi-Zenith Satellite System (QZSS) and the Indian Regional Satellite Navigation System (IRNSS/NAVIC).

2.2 Spatial Reference Systems

To establish coordinates of points requires that we set up a coordinate system with origin, orientation, and scale defined in such a way that all users have access to these. Before the establishment of GNSS, the most accessible reference for coordinates from a global perspective was the celestial sphere of stars that were used not only for charting and navigation, but also served as a fundamental system to which other terrestrial coordinate systems could be oriented. Still today, the celestial reference system is used for that purpose and may be thought of as the ultimate in reference systems. At the next level, we define coordinate systems attached to the Earth with various origins (and perhaps different orientations and scale). Thus, there are two fundamental tasks: (1) to establish an external coordinate system of the local universe that presumably remains fixed in the sense of no rotation; and (2) to establish a coordinate system attached to the rotating and orbiting Earth, and in so doing to find the relationship between these two systems.

2.2.1 Coordinate Systems

The Cartesian system of coordinates, x, y, z, is certainly the easiest from a mathematical perspective and it plays a central role in defining modern reference systems. However, because the Earth is nearly spherical and by extension our geocentric view of the heavens takes on a spherical character, spherical coordinates are essential as many geodetic concepts rely on directions and distances. Indeed, the latitude/longitude concept will always have the most direct appeal for terrestrial applications (surveying, near-surface navigation, positioning, and mapping). Figure 2.5 shows the relationship between the Cartesian coordinates and *spherical coordinates*, comprising latitude, ϕ, longitude, λ, and radius, r, and given by

$$\begin{aligned} x &= r\cos\phi\cos\lambda\,, \\ y &= r\cos\phi\sin\lambda\,, \\ z &= r\sin\phi\,. \end{aligned} \tag{2.14}$$

The inverse relationship is

$$\begin{aligned} \phi &= \tan^{-1}\left(\frac{z}{\sqrt{x^2+y^2}}\right), \\ \lambda &= \tan^{-1}\left(\frac{y}{x}\right), \\ r &= \sqrt{x^2+y^2+z^2}\,. \end{aligned} \tag{2.15}$$

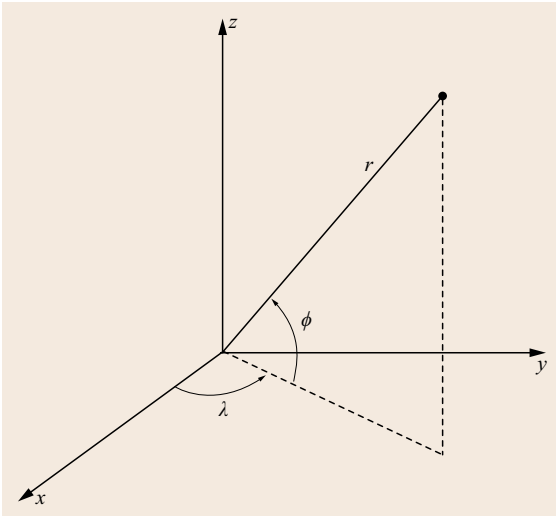

Fig. 2.5 Spherical coordinates

Already by the middle of the eighteenth century, it was established by measurements that the Earth is flattened at the poles and assumes an elliptical shape [2.30], specifically an *ellipsoid* of revolution, defined as the surface generated by rotating an ellipse about its minor axis. It is also known as a *spheroid* (to distinguish it from a tri-axial ellipsoid). Essential parameters of the ellipsoid are its size and shape that may be defined by the semi-major and semi-minor axis lengths, a and b (Fig. 2.6). Other shape parameters include the flattening

$$f = \frac{a-b}{a} \,, \tag{2.16}$$

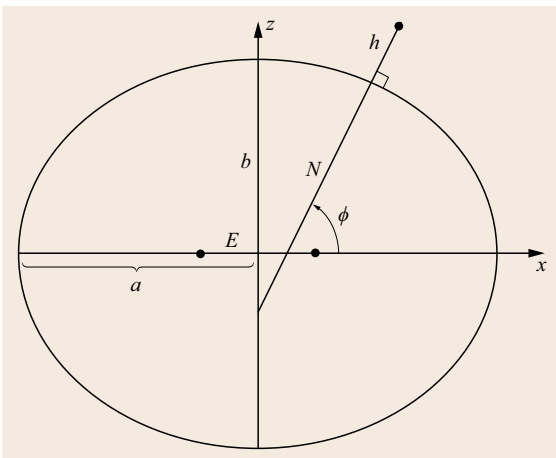

Fig. 2.6 Ellipsoidal geometry and geodetic coordinates. *Dots* on the x-axis denote focal points of the ellipse, which represents the meridian plane

the first and second eccentricities

$$e^2 = \frac{a^2-b^2}{a^2} \quad \text{and} \quad e'^2 = \frac{a^2-b^2}{b^2} \,, \tag{2.17}$$

as well as the linear eccentricity $E = ae$.

With respect to an ellipsoid with given parameters, the *geodetic coordinates* are defined as illustrated in Fig. 2.6 and include the geodetic latitude, φ, the geodetic longitude, λ (not shown, but identical to the spherical longitude), and the geodetic height, h, along the line that is normal, or perpendicular, to the ellipsoid. The relationship between geodetic coordinates and the global Cartesian coordinates is

$$\begin{aligned} x &= (N+h)\cos\varphi\cos\lambda \,, \\ y &= (N+h)\cos\varphi\sin\lambda \,, \\ z &= \left[N\left(1-e^2\right)+h\right]\sin\varphi \,, \end{aligned} \tag{2.18}$$

where

$$N = \frac{a}{\sqrt{1-e^2\sin^2\varphi}} \,. \tag{2.19}$$

is the radius of curvature of the ellipsoid in the direction perpendicular to the elliptical meridian plane.

An inverse relationship can be formulated for $z \neq 0$ that requires a numerical iteration on the geodetic latitude,

$$\varphi = \tan^{-1}\left[\frac{z}{\sqrt{x^2+y^2}}\left(1+\frac{e^2N\sin\varphi}{z}\right)\right] , \tag{2.20}$$

where the initial latitude that assumes the point is on the ellipsoid ($h = 0$),

$$\varphi^{(0)} = \tan^{-1}\left[\frac{z}{\sqrt{x^2+y^2}}\left(1+\frac{e^2}{1-e^2}\right)\right] , \tag{2.21}$$

serves to yield convergence to micro-arcsecond accuracy within three iterations for heights less than 20 km. The height then follows from

$$h = \left(\sqrt{x^2+y^2}\right)\cos\varphi + z\sin\varphi \; - a\sqrt{1-e^2\sin^2\varphi} \,, \tag{2.22}$$

and the longitude is given by the second equation of (2.15).

A noniterative relationship is derived by [2.31] based on the solution to a quartic equation; see also [2.32]. The performance and computational efficiency of different analytical and iterative algorithms

for the conversion of Cartesian to geodetic coordinates is, furthermore, compared in [2.33].

A number of ellipsoids have been established on the basis of geodetic measurements, extending historically from surveyed arc lengths along meridians to modern best fits to mean sea level using satellite altimetry. One of the earliest ellipsoids was computed by Airy in 1830, having semi-major axis, $a = 6\,377\,563.396\,\mathrm{m}$, and flattening, $f = 1/299.324964$. The current internationally adopted ellipsoid is part of the Geodetic Reference System of 1980 (GRS80) and has parameter values given by

$$a_{\mathrm{GRS80}} = 6\,378\,137\,\mathrm{m}\,,$$
$$f_{\mathrm{GRS80}} = \frac{1}{298.257222101}\,. \tag{2.23}$$

The equatorial radius was determined from satellite altimetry and the flattening was derived from the second-degree zonal harmonic coefficient (dynamic form factor, J_2) of the Earth's gravitational potential [2.34]. The parameter values of other ellipsoids determined and used in the past may be found in [2.30]. The parameter estimates of the best fitting, or mean Earth ellipsoid (MEE) in the mean tide system are [2.35]

$$a_{\mathrm{MEE}} = 6\,378\,136.72 \pm 0.1\,\mathrm{m}\,,$$
$$f_{\mathrm{MEE}} = \frac{1}{298.25231 \pm 0.00001}\,. \tag{2.24}$$

The GRS80 values are constants, while the MEE values are estimates with a standard deviation and do not constitute an accepted reference ellipsoid. When publishing geodetic coordinates, φ, λ, h, it is always important to specify the associated ellipsoid on which they depend.

Local coordinates in the vicinity of a point P are Cartesian with the third axis along the ellipsoid normal

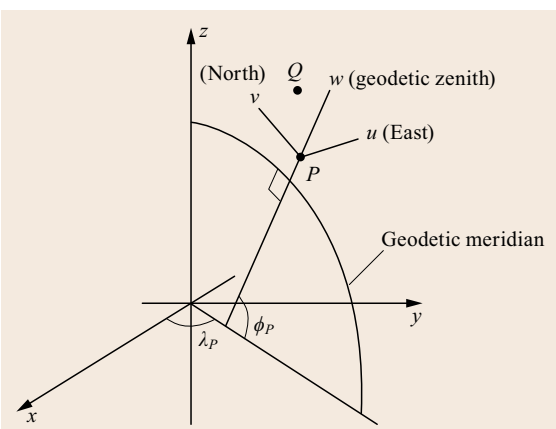

Fig. 2.7 Local Cartesian coordinates, u, v, w

as illustrated in Fig. 2.7. For a right-handed system, the first axis points East and the second North. However, a left-handed system, such as North-East-Up, is also common. Local coordinates $(u, v, w)^\top$ of a point Q in a system centered at P are related to the global Cartesian coordinate differences $(\Delta x, \Delta y, \Delta z)^\top$ of Q with respect to P according to

$$\begin{pmatrix} u \\ v \\ w \end{pmatrix} = \mathbf{E} \begin{pmatrix} \Delta x \\ \Delta y \\ \Delta z \end{pmatrix} \tag{2.25}$$

with

$$\mathbf{E} = \begin{pmatrix} -\sin\lambda & +\cos\lambda & 0 \\ -\sin\varphi\cos\lambda & -\sin\varphi\sin\lambda & +\cos\varphi \\ +\cos\varphi\cos\lambda & +\cos\varphi\sin\lambda & +\sin\varphi \end{pmatrix}. \tag{2.26}$$

Here, the latitude φ and longitude λ refer to the reference point P. The inverse relationship is obtained by premultiplying both sides by the transpose of the rotation matrix since it is orthogonal.

The elevation angle E of Q relative to P and the corresponding azimuth angle A (measured clockwise from North to East) are given by

$$\tan A = \frac{u}{v}$$
$$\sin E = \frac{w}{\sqrt{u^2 + v^2 + w^2}}\,. \tag{2.27}$$

These formulas relate global Cartesian coordinate differences, as might be obtained by GNSS, to local determinations of angles and distances. If those angles are referenced to the local plumb line, rather than the ellipsoidal normal, one needs to account for this *deflection of the vertical*. For a distance of 1 km and a vertical deflection of 30″, the effect on the global Cartesian coordinate differences is of the order of a few centimeters or decimeters.

Celestial coordinates refer to the location of objects (e.g., stars) projected onto the *celestial sphere*. By definition, the celestial sphere has no particular radius as the coordinates define only directions. The center of the sphere is defined to be at the origin of a Cartesian coordinate system, and the celestial coordinates are called declination (δ) and right ascension (α), analogous to latitude and longitude. As such, the relationship to Cartesian coordinates is the same as in (2.14) and (2.15) with unit radius ($r = 1$). The origins for declination and right ascension require particular definitions associated with a reference system. This is discussed further in Sect. 2.4.

2.2.2 Reference Systems and Frames

There is an important conceptual difference between a reference system for coordinates and a reference frame that applies throughout the discussion of coordinate systems in geodesy. Loosely recognized in defining and creating geodetic datums in the past, it was formalized by [2.36] (see also [2.37, Chap. 9] and [2.6]):

- A *reference system* is a set of prescriptions and conventions together with the modeling required to define at any time a triad of coordinate axes.
- A *reference frame* realizes the system by means of coordinates of definite points that are accessible directly by occupation or by observation.

A simple example of a reference system is the set of three mutually orthogonal axes that are aligned with the Earth's spin axis, a prime (Greenwich) meridian, and a third direction orthogonal to these two in the right-handed sense. That is, a system defines how the axes are to be established (e.g., orthogonality), what theories or models are to be used (e.g., what is meant by a spin axis), and what conventions are used (e.g., how the prime meridian is to be chosen). A simple example of a frame is a set of points globally distributed whose coordinates are given mutually consistent numbers in the reference system. That is, a frame is the physical realization of the system defined by actual coordinate values of actual points in space that are accessible to anyone. A frame cannot exist without a system, and a system is of no practical value without a frame.

Although the explicit difference between frame and system was articulated fairly recently in geodesy, the concepts have been embodied in the terminology of a *geodetic datum* that can be traced to the eighteenth century and earlier [2.30]. Indeed, the definition of a datum today refers specifically to the conventions that establish how a coordinate system is attached to the Earth – its origin, its orientation, and its scale. In this sense, the definition of a datum has not changed. The meaning of a datum within the context of frames and systems is explored in more detail in Sect. 2.3.2.

2.3 Terrestrial Reference System

Geodetic control at local, regional, national, and international levels has been revolutionized by the advent of satellite systems, particularly GNSS that provide accurate positioning capability to terrestrial observers at all scales, where, of course, the GPS has had the most significant impact. The terrestrial reference systems and frames for geodetic control have evolved correspondingly over the last few decades. Countries and continents around the world are revising, redefining, and updating their fundamental networks to take advantage of the high accuracy, the ease of establishing and densifying the control, and critically important, the uniformity of the accuracy and the connectivity of the control that can be achieved basically in a global setting.

2.3.1 Traditional Geodetic Datums

The traditional *geodetic datum* was defined somewhat loosely by today's standards as a set of constants and prescriptions that specify a coordinate system for the purpose of geodetic control [2.38]. Because of the fundamental differences in respective measurement techniques, control was divided between horizontal and vertical datums.

Horizontal datums (Fig. 2.8) required the definition of an origin point (a marker on the Earth's surface with defined geodetic latitude and longitude; or, equivalently, a constraint within a network that essentially fixed the origin), as well as a mapping surface, an ellipsoid with defined parameters. Orientation of the ellipsoid was defined to be parallel to the astronomic system of the celestial sphere (Sect. 2.4). It was realized by accurate measurements of azimuth with respect to celestial north and by accounting for the deflection of the vertical in astronomic determinations of coordi-

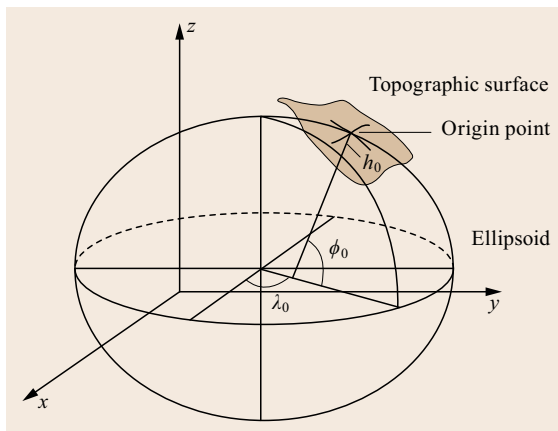

Fig. 2.8 Traditional horizontal geodetic datum. Geodetic surveys on the topographic surface relative to an origin point are reduced to a mapping surface, the ellipsoid, with proper preservation of its orientation relative to an astronomic system

nates. A *vertical datum* (Fig. 2.9) was similarly defined by the height at an origin point and prescriptions for the reference surface through that point and the associated heights relative to the surface.

In the United States, horizontal control was established in the latter half of the nineteenth century for the Eastern United States and advanced with the westward economic expansion to create the *North American Datum of 1927* (NAD27) with origin point at Meades Ranch in the centrally located state of Kansas. In 1983, the horizontal datum was redefined to be geocentric (origin at the now practically accessible center of mass of the Earth by tracking Earth-orbiting satellites), referred to the GRS80 ellipsoid, and readjusted with the inclusion of satellite Doppler observations and other space techniques such as very long baseline interferometry (VLBI [2.39, 40]). The new *North American Datum of 1983* (NAD83), already incorporating three-dimensional coordinates, assumed a fully three-dimensional character with each new realization that was adjusted by including continuously operating reference stations (CORS [2.41]). The CORS network is a cooperative endeavor among the US government (National Geodetic Survey) and academic and private institutions that creates precise geodetic control throughout the United States and several worldwide stations using GNSS data. New realizations of NAD83 were adjusted as the CORS network expanded and were designated NAD83(CORS93), NAD83(CORS94), and NAD83(CORS96). Including also additional regional high-accuracy GPS networks that were adjusted to fit the NAD83(CORS96) frame, it became the geometric part of the National Spatial Reference System, designated NAD83(NSRS2007). This was readjusted in 2011, yielding the realization NAD83(2011) with coordinates and their velocities (Sect. 2.3.4) given for the epoch $t_0 = 2010.0$. The reference system definition is currently (2015) in revision to bring the realization closer to the International Terrestrial Reference Frame (ITRF) (Sect. 2.3.2).

The vertical datum in the United States similarly evolved from an adjustment of coast-to-coast leveling networks constrained to zero height at various tide-gauge stations at mean sea level. This *National Geodetic Vertical Datum of 1929* (NGVD29) was replaced in 1988 with a readjustment of existing and new leveling data and a tie to the *International Great Lakes Datum of 1985* (IGLD85) whose origin is a single point on the St. Lawrence River in the province of Québec, resulting in the *North American Vertical Datum of 1988* (NAVD88). Vertical control in the United States and Canada is now undergoing a fundamental redefinition to eliminate continent-wide error trends by defining the reference, not by any particular origin point, but by a model for the Earth's gravity potential. This new *geopotential reference system* already exists for Canada as of 2013, and is scheduled to be in place for the United States by the early 2020s.

Similar progress in geodetic control is occurring in other regions of the world, for example, in Europe and South America, where in some cases progress is more difficult due to the varied and heterogeneous datums established in the pre-satellite era.

While geodetic control is now essentially three-dimensional within a single reference system and frame, such as NAD83(NSRS2007), vertical datums continue to be vitally important since they define a different kind of height, one that is based on gravity potential, rather than pure geometry. The geopotential-based heights are needed for any application in hydrology since they indicate the natural flow of water.

The conversion between ellipsoidal heights, h, obtained from coordinates in the modern geodetic reference system and heights, H, in a vertical datum requires a model for the *geoid undulation*, or *geoid height*, N, defined as the vertical separation between the geoid and the ellipsoid (Fig. 2.10)

$$N = h - H - N_0 \,. \tag{2.28}$$

The *geoid* is the equipotential surface that closely approximates global mean sea level and the geoid undulation is determined from gravity measurements [2.42]. High-degree and high-order spherical harmonic gravitational potential models such as EGM2008 can provide global geoid undulations with an accuracy of 10 cm or better as shown in [2.43]. In addition, a constant offset, N_0, must be determined between the geoid and the ver-

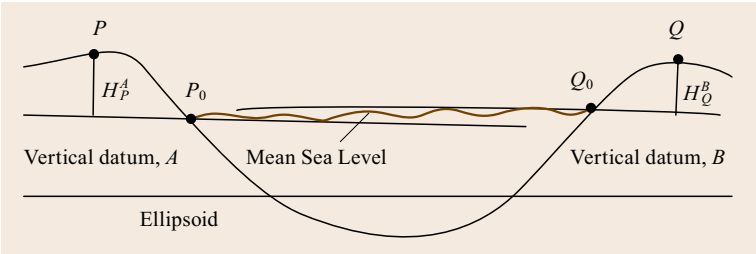

Fig. 2.9 Traditional vertical geodetic datum, representing an equipotential, or level, surface in Earth's gravity field. Since mean sea level is not truly level, different vertical datums tied to mean sea level are not mutually consistent

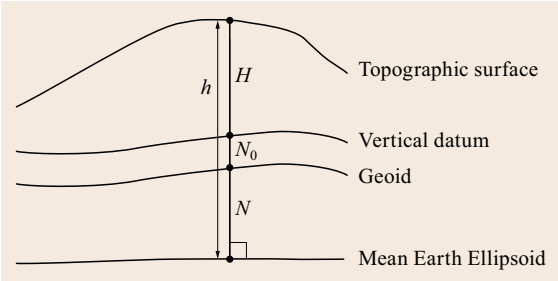

Fig. 2.10 The relationship between heights with respect to a vertical datum and the ellipsoid

tical datum, as well as a possible difference between the best-fitting MEE and the ellipsoid of the reference system. This offset can reach several decimeters in value.

The geoid undulation itself covers a range of roughly ±100 m with positive peak values in the North Atlantic and Indonesian region and a minimum near the Southern tip of India (Fig. 2.11). GNSS do not have direct access to geoid-related (mean sea level) heights but can only obtain the height with respect to a reference ellipsoid from the navigation solution. For conversion of ellipsoidal heights to mean sea level, a database of precomputed geoid undulations can be used within a GNSS receiver. As an example, [2.44] provides tabular geoid heights on a 10° × 10° longitude/latitude grid. The geoid height at any user location can then be obtained through interpolation using a weighted average of the nearest four grid points with a root-mean-square accuracy of better than 4 m. Higher accuracy would require a finer grid and a more accurate geoid model, such as EGM2008.

2.3.2 Global Reference System

The definition of a global terrestrial reference system (or, *terrestrial reference system*, TRS) began in earnest with the advent of Earth-orbiting satellites that enabled a realization of the center of mass and thus a natural origin for the coordinate system. Other names are conventional terrestrial reference system and geocentric terrestrial reference system. The roots of efforts to define a global system, however, can be traced back to the turn of the last century. In 1899, the *International Latitude Service* (ILS) was established by the *International Association of Geodesy* (IAG) to conduct astronomic latitude observations that monitor the motion of Earth's rotation axis relative to the Earth (polar motion, Sect. 2.5.3). By observing and disseminating this motion, latitudes and longitudes obtained by observing the stars could be corrected so that they refer to a fixed global terrestrial system.

In 1960, it was decided at the General Assembly of the *International Union of Geodesy and Geophysics* (IUGG) to adopt as terrestrial pole the average of the

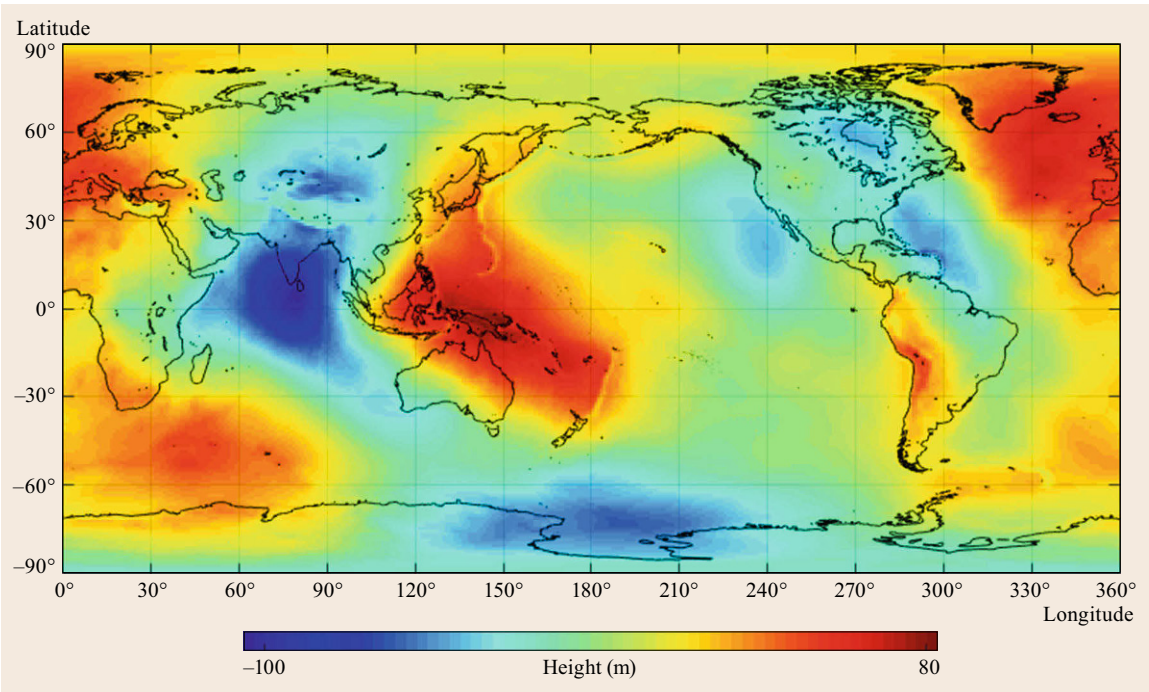

Fig. 2.11 Geoid heights relative to the Earth ellipsoid (courtesy of Th. Fecher)

positions of the true celestial pole on the Earth during the period 1900–1905 (a 6 year period over which the Chandler period of 1.2 years would repeat five times; Sect. 2.5.3). This average was named the *Conventional International Origin* (CIO).

The global reference meridian, or, origin for longitudes, originally defined astronomically as the meridian through the Greenwich observatory, near London, England, was realized by an average, as implied by the longitudes of many observatories around the world, corrected for polar motion and length-of-day variations.

These early conventions and procedures to define and realize a terrestrial reference system addressed astronomic *directions* only; no attempt was made to define a realizable origin, although implicitly it could be considered as geocentric. In 1984, the BIH, responsible until this time for monitoring the pole and the Greenwich meridian, defined the BIH Conventional Terrestrial System (CTS) (or also BTS) based on satellite laser ranging (SLR), VLBI, and other space techniques. With the inclusion of satellite observations, an (indirectly) accessible geocentric origin of the system could now be defined. New and better satellite and VLBI observations became available from year to year, and the BIH published new realizations of its system: BTS84, BTS85, BTS86, and BTS87. With the orientation of the TRS now defined by geometric satellite and space observations, the origin of geodetic longitudes, to be consistent with its astronomic counterpart (maintained for continuity in time keeping), is now about 102 m to the east of the Greenwich Observatory, which accounts for the local deflection of the vertical [2.45].

In 1988, the functions of monitoring the pole and the reference meridian were turned over to the newly established *International Earth Rotation Service* (IERS). The time service, originally also under the BIH, now resides with the BIPM. The new reference pole realized by the IERS, called the *International Reference Pole* (IRP), was adjusted to fit the BIH reference pole of 1967 – 1968 and presently is consistent with the CIO to within $\pm 0.03''$ (1 m).

The IERS, renamed in 2003 to *International Earth Rotation and Reference Systems Service* (retaining the same acronym), is responsible for defining and realizing both the *International Terrestrial Reference System* (ITRS) and the *International Celestial Reference System* (ICRS). In each case, an origin, an orientation, and a scale are defined among other conventions for the system. The system is then realized as a frame by the specification of these datum parameters and the coordinates of points worldwide. Since various observing systems (analysis centers and techniques) contribute to the overall realization of the reference system and since new realizations are obtained recurrently with improved observation techniques and instrumentation, the transformations among various realizations of the system are of paramount importance. Especially, if one desires to combine data referring to realizations of different reference systems, or to different realizations of the same system, it is important to understand the coordinate relationships so that the data are combined ultimately in one consistent coordinate system.

The ITRS is defined by an orthogonal triad of right-handed, equally scaled axes with the following additional conventions:

1. The *origin* is geocentric, that is, at the center of mass of the Earth (including the mass of the oceans and atmosphere). Because measurement precision has reached the level of detecting variations in the center of mass due to terrestrial mass redistributions, the origin is defined as an average location of the center of mass and referred to an epoch.
2. The *scale* is defined by the SI meter, which is based on an adopted speed of light in vacuum and is connected to the definition of the SI second (Sect. 2.1).
3. The *orientation* is defined by the directions of the IRP and the reference meridian as given for 1984 by the BIH. Since it is now well established that Earth's crust (on which observing stations are located) is divided into tectonic plates that exhibit motion of the order of centimeters per year, it is further stipulated that the time evolution of the orientation of the reference system has no residual global rotation with respect to the crust (*no-net-rotation* condition). That is, even though the points on the crust, through which the system is realized, move with respect to each other, the net rotation of the system with respect to its initial definition should be zero.

The realization of the ITRS is the *International Terrestrial Reference Frame* (ITRF) and requires that three origin parameters, three orientation parameters, and a scale parameter must be identified with actual values. Each new ITRF of the system is named with the year that corresponds to the last available data incorporated in its realization. As of this writing (2015), the latest frame is ITRF2008 [2.46], and ITRF2013 is in preparation. The seven parameters are not observable without conventions (see below) and their specification is formulated by the IERS in terms of constraints imposed on the solution of coordinates from observations. Moreover, the constraints are cast in the form of a seven-parameter similarity transformation (commonly known as *Helmert* transformation) *from* an a priori given frame *to* the realized frame. The seven parameters include three translation parameters, T_i, that realize the origin; three

angle parameters, R_i, that realize the orientation; and, a scale change parameter, D, that realizes the scale

$$\begin{pmatrix} x \\ y \\ z \end{pmatrix}_{\text{to}} = \begin{pmatrix} x \\ y \\ z \end{pmatrix}_{\text{from}} + \begin{pmatrix} T_1 \\ T_2 \\ T_3 \end{pmatrix} + D \begin{pmatrix} x \\ y \\ z \end{pmatrix}_{\text{from}} + \begin{pmatrix} 0 & -R_3 & +R_2 \\ +R_3 & 0 & -R_1 \\ -R_2 & +R_1 & 0 \end{pmatrix} \begin{pmatrix} x \\ y \\ z \end{pmatrix}_{\text{from}} \tag{2.29}$$

where the translation and rotation parameters are defined in Fig. 2.12. For example, if the origin of an existing frame is known to be the geocenter, then the next realization, based on new observations, can be related to the previous frame by constraining the translation to be zero. The transformation given by (2.29) is a linear approximation where, because of the small values of the transformation parameters, the neglect of second- and higher order terms affects coordinates at the subnanometer level.

Because these datum (transformation) parameters are determined for points on the Earth's crust (*crust-based frame*), and because the Earth as a whole is a dynamic entity, the parameters are associated with an epoch, t_0, and, today, are supplemented with rates of change, making the total number of parameters equal to 14. Thus, the i-th transformation parameter, β_i, is a function of time,

$$\beta_i(t) = \beta_{0,i} + \dot{\beta}_{0,i}(t - t_0)\,, \tag{2.30}$$

and the 14 parameters are $\beta_{0,i}$ and $\dot{\beta}_{0,i}$ with $i = 1, \ldots, 7$.

Whether the origin of a coordinate system is implied by a marker on the Earth's surface or accessed via distance measurements to Earth-orbiting satellites, it is defined by a convention, just like all other parts of the coordinate system. As such it is not, a priori, an observable quantity like a distance or an angle. This is the classic *datum defect* problem, well known in all types of surveying, where observations of distances and angles must ultimately be *related* to a point or direction that is fixed or defined by convention.

With satellite techniques, on the other hand, there is the advantage of knowing that the center of mass is the centroid for all orbits. Hence, the center of mass of the Earth serves as a natural origin point that, in theory, is accessible. That is, if the orbit is known, distance observations from points on the Earth's surface to points on the orbit are in a geocentric system, by definition. Due to observational error not all origin realizations, however, are identical as obtained by different analysis centers that, moreover, process different satellite data (such as satellite and lunar laser ranging [2.47, 48], GNSS [2.49], and Doppler data [2.50]). Generally, the most precise methods are based on SLR.

For the first ITRFs in the early 1990s, it was customary to relate all frames realized by particular analysis centers and/or satellite techniques to one of the SLR solutions from the Center for Space Research (CSR) in Austin, Texas, which was considered to be the best solution that accesses the center of mass and thus realizes the origin. The origins of solutions (i. e., realized coordinate systems) from other techniques, such as Doppler and GPS, were related by IERS to the ITRF origin through a translation determined by using stations that are common to both the CSR and the other solutions. For later ITRFs, a weighted average of selected SLR and GPS solutions was used to realize the origin. The origin of ITRF2000 was realized by a weighted average of *the most consistent SLR solutions* submitted to the IERS. With ITRF2005 and ITRF2008, the IERS used a time series over 13 years and 26 years, respectively, of reprocessed SLR data at selected, globally distributed sites to realize the origin.

Similarly, the scale was realized for the early ITRFs by the SLR solutions from the CSR analysis center, with the scale of other solutions transformed accordingly. For later realizations of scale, SLR was combined with VLBI, which accurately determines coordinate

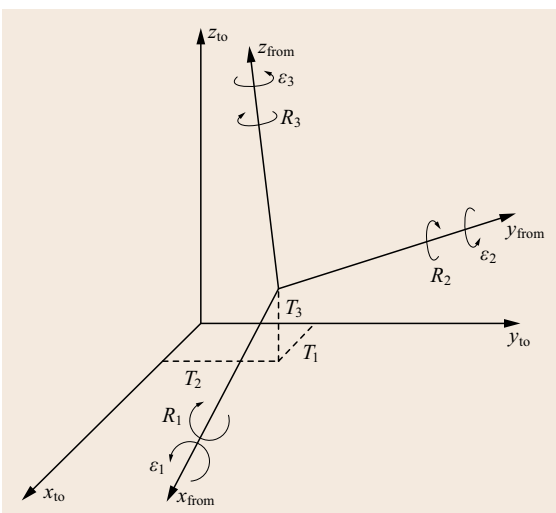

Fig. 2.12 Transformation parameters between coordinate frames. The similarity transformation (2.29) yields the coordinates of a point in a new frame $\mathcal{R}_{\text{to}}$ that originates from the old frame $\mathcal{R}_{\text{from}}$ through translation of the origin by $-T_i$ ($i = 1, 2, 3$) and a *left*-handed rotation about the i-th axis by angle R_i. Rotation angles R_i comply with IERS conventions, whereas rotation angles $\varepsilon_i = -R_i$ (corresponding to right-handed rotations), are used by the US National Geodetic Survey

differences of stations separated by large distances (several 1000 km) using observed directions to quasars [2.6, Chap. 4.2.2].

Satellite and space observational techniques contain no information on the absolute longitudinal orientation of a system. This orientation has no obvious natural reference and is completely arbitrary (the Greenwich meridian). One might argue that the orientation of the equatorial plane (or, equivalently, the polar direction), like the center of mass, is a natural reference that is accessible indirectly from astronomic observations, VLBI, and satellite tracking. However, the polar direction is complicated, a result of both polar motion with respect to the Earth's crust (Sect. 2.5.3), and precession and nutation with respect to the celestial sphere (Sect. 2.5.1). Besides this, the stations on the Earth's crust, which ultimately realize the ITRS, are in constant motion due to plate tectonics. Thus, the adopted convention for realizing the orientation of the ITRS is to ensure that each successive realization after 1984 is aligned with the orientation defined by the BIH in 1984 (with some early adjustments for different solutions of the Earth orientation parameters (Sect. 2.5.1)).

The methods of combining different solutions and introducing the constraints needed to address the datum defect (i. e., specifying origin, scale, and orientation) have become increasingly complicated as more data are assimilated and analysis centers employ different weighting schemes to account for the various observational accuracies. Relevant details may be found in the IERS Conventions of 2003 and 2010 and references therein, specifically also publications by [2.51, 52] and their references.

The model for the coordinates of any of the observing stations participating in the realization of ITRS is given by

$$\boldsymbol{x}(t) = \boldsymbol{x}_0 + (t - t_0)\boldsymbol{v}_0 + \sum_i \Delta\boldsymbol{x}_i(t) \,, \tag{2.31}$$

where $\boldsymbol{x}_0$ and $\boldsymbol{v}_0$ are the vectors of the coordinates of the observing station and its velocity, defined for a particular epoch, t_0. These are solved on the basis of observed coordinates, $\boldsymbol{x}(t)$, at time, t, using some type of observing system (e.g., SLR). The quantities, $\Delta\boldsymbol{x}_i$, are corrections applied by analysis centers to account for various, short wavelength, local geodynamic effects, such as solid Earth tides, ocean loading, and atmospheric loading (Sect. 2.3.5), with the objective of accounting for the nonconstant velocities. Details for the corresponding recommended models are provided by the IERS Conventions 2010 [2.6, Chap. 7]. The coordinate vector, $\boldsymbol{x}_0$, and the linear velocity, $\boldsymbol{v}_0$, for each participating station is provided by IERS as a result of the assimilation of all data, and these represent the consequent realization of ITRS at epoch t_0.

In the past, the linear velocity was modeled largely by the NNR-NUVEL1A tectonic plate motion model [2.32, 53, 54]. Thus,

$$\boldsymbol{v}_0 = \boldsymbol{v}_{\mathrm{NUVEL1A}} + \delta\boldsymbol{v}_0 \,, \tag{2.32}$$

where $\boldsymbol{v}_{\mathrm{NUVEL1A}}$ is the velocity given as a set of rotation rates for the major tectonic plates, and $\delta\boldsymbol{v}_0$ is a residual velocity for the station. The major tectonic plates and site velocities predicted from a plate motion model are illustrated in Fig. 2.13. The newest ITRFs (since ITRF2000) appear to indicate significant departures of the station velocities $\boldsymbol{v}_0$ from the NNR-NUVEL1A model [2.55], which, however, does not impact the integrity of the ITRF.

2.3.3 Terrestrial Reference Systems for GNSS Users

The various navigation satellite systems have adopted specific reference systems for the provision of orbit information to their users. While the associated realizations may traditionally exhibit small offsets with respect to each other, GNSS providers are making continued effort to align the respective realizations with current versions of the ITRF.

In case of the US Global Positioning System, the World Geodetic System 1984 (WGS84, [2.56]) serves as the basis for orbit determination and broadcast ephemeris generation in the GPS control segment. WGS84 is the equivalent of the ITRS for the US Department of Defense (and includes also a global gravitational model). It is the evolution of previous reference systems, WGS60, WGS66, and WGS72 [2.57]. The corresponding reference frame for WGS84, as originally realized in 1987 on the basis mostly of satellite Doppler observations, agreed approximately with NAD83. The next realization, designated WGS84(G730), made use of observations from 12 GPS stations around the world and was aligned with the ITRF92 to an accuracy of about 20 cm in all coordinates. Here, G730 refers to GPS week 730 (Jan. 1994), the reference epoch of the WGS84 realization. Subsequent versions, known as WGS84(G873), WGS84(G1150) [2.58], and WGS84(G1674) [2.59], achieved continual improvements and are consistent, respectively, with ITRF94, ITRF2000, and ITRF2008 at the level of 10, 2, and 1 cm accuracy.

For the Russian Global'naja Nawigatsionnaja Sputnikowaya Sistema (GLONASS), the PZ-90 (Parametry Zemli – 90) system is employed. PZ-90 follows the same principles as the ITRS and WGS84, but is realized

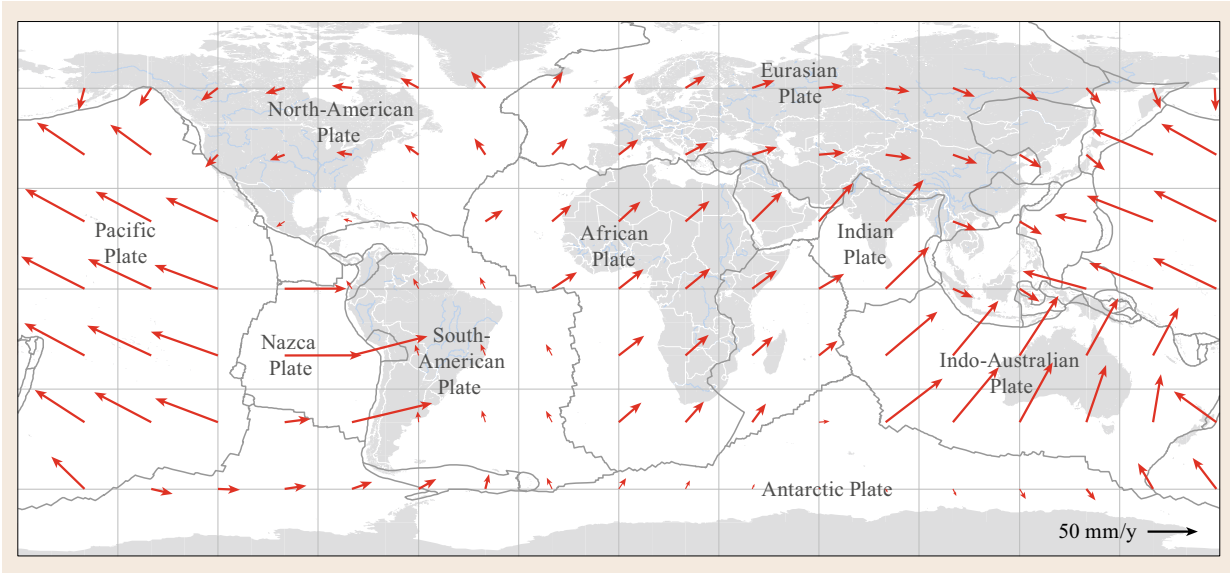

Fig. 2.13 Tectonic plates and predicted site velocities

through different reference stations and measurements. While the initial release of PZ-90 exhibited meter-level offsets from WGS84, the consitency was notably improved in 2007 with introduction of PZ-90.2 [2.60]. In early 2014, the GLONASS Control Segment finally switched to PZ-90.11 [2.61, 62], which offers a centimeter-level agreement with the latest ITRF versions.

Next to WGS84 and PZ-90, independent reference systems/frames are also employed for the BeiDou (China Geodetic Coordinate System 2000, CGS2000 [2.63]) as well as the European Galileo navigation system (Galileo Terrestrial Reference Frame, GTRF [2.64]).

2.3.4 Frame Transformations

The parameters of the Helmert similarity transformation (2.29) are determined in a weighted least-squares adjustment of the transformation model for the differences between coordinates of the same points in two frames. Table 2.2 lists the transformation parameters among the various IERS (and BIH) terrestrial reference frames since 1984. Due to the linear nature of the transformation, the reverse transformation is obtained by simply reversing the signs of the parameters. Also, the parameter values for a transformation between nonsuccessive frames are simply the accumulated values between the frames. However, especially for the later frames, the epoch of their validity must be considered. Rates of the parameters are given only since 1993 and (2.30) yields transformation parameters for other than the listed epoch. Using the last row of Table 2.2 as an example, the translation in x between ITRF2005 and ITRF2008 at the epoch $t = 2000.0$ is given by

$$\begin{aligned} T_1(t) &= T_1(t_0) + \dot{T}_1 \cdot (t - t_0) \\ &= 0.05\,\mathrm{cm} - 0.03\,\mathrm{cm/y} \cdot (-5\,\mathrm{y}) \\ &= 0.20\,\mathrm{cm}\,. \end{aligned} \tag{2.33}$$

On the other hand, each of the determined parameters also has an associated uncertainty (given by the IERS, but not listed in Table 2.2, which should be properly included in any such calculation).

Table 2.3 lists transformation parameters from the original realization of WGS84 to ITRF90 as published by the IERS [2.65], as well as from recent ITRFs to NAD83(CORS96) as published by the National Geodetic Survey [2.67]. There is no origin, scale, and orientation change between NAD83(2011) and NAD83(CORS96). Again, uncertainties in the parameters are not listed. Also, the more recent realizations WGS84 are essentially equivalent to the correspondingly contemporary ITRF (Sect. 2.3.3).

Resolutions 1 and 4 of the 1991 IAG General Assembly [2.68] recommend that regional high-accuracy reference frames be tied to an ITRF, where such frames associated with large tectonic plates may be allowed to rotate with these plates as long as they coincide with an ITRF at some epoch. This procedure was adopted for NAD83, which for the conterminous United States and Canada lies (mostly) on the North American tectonic plate. This plate has global rotational motion estimated

Table 2.2 Transformation parameters among ITRF and BTS frames for use with the 7/14-parameter Helmert model (2.29) and (2.30). Time-dependent transformation parameters are provided from ITRF93 onward. Based on data from [2.6, 65, 66]

From	To	$T_1\|\dot{T}_1$ (cm) (cm/y)	$T_2\|\dot{T}_2$ (cm) (cm/y)	$T_3\|\dot{T}_3$ (cm) (cm/y)	$R_1\|\dot{R}_1$ (0.001″) (0.001″/y)	$R_2\|\dot{R}_2$ (0.001″) (0.001″/y)	$R_3\|\dot{R}_3$ (0.001″) (0.001″/y)	$D\|\dot{D}$ (10^{-8}) (10^{-8}/y)	t_0
BTS84	BTS85	+5.4	+2.1	+4.2	−0.9	−2.5	−3.1	−0.5	1984
BTS85	BTS86	+3.1	−6.0	−5.0	−1.8	−1.8	−5.81	−1.7	1984
BTS86	BTS87	−3.8	+0.3	−1.3	−0.4	+2.5	+7.5	−0.2	1984
BTS87	ITRF0	+0.4	−0.1	+0.2	0.0	0.0	−0.2	−0.1	1984
ITRF0	ITRF88	+0.7	−0.3	−0.7	−0.3	−0.2	−0.1	+0.1	1988
ITRF88	ITRF89	+0.5	+3.6	+2.4	−0.1	0.0	0.0	−0.31	1988
ITRF89	ITRF90	−0.5	−2.4	+3.8	0.0	0.0	0.0	−0.3	1988
ITRF90	ITRF91	+0.2	+0.4	+1.6	0.0	0.0	0.0	−0.03	1988
ITRF91	ITRF92	−1.1	−1.4	+0.6	0.0	0.0	0.0	−0.14	1988
ITRF92	ITRF93	−0.2	−0.7	−0.7	−0.39	+0.80	−0.96	+0.12	1988
		−0.29	+0.04	+0.08	−0.11	−0.19	+0.05	0.0	
ITRF93	ITRF94	−0.6	+0.5	+1.5	+0.39	−0.80	+0.96	−0.04	1988
		0.29	−0.04	−0.08	+0.11	+0.19	−0.05	0.0	
ITRF94	ITRF96	0.0	0.0	0.0	0.0	0.0	0.0	0.0	1997
		0.0	0.0	0.0	0.0	0.0	0.0	0.0	
ITRF96	ITRF97	0.0	0.0	0.0	0.0	0.0	0.0	0.0	1997
		0.0	0.0	0.0	0.0	0.0	0.0	0.0	
ITRF2000	ITRF2005	−0.01	+0.08	+0.58	0.0	0.0	0.0	−0.040	2000
		+0.02	−0.01	+0.18	0.0	0.0	0.0	−0.008	
ITRF2005	ITRF2008	+0.05	+0.09	+0.47	0.0	0.0	0.0	−0.094	2005
		−0.03	0.00	0.00	0.0	0.0	0.0	0.0	

Table 2.3 Transformation parameters for other terrestrial reference frames for use with the 7/14-parameter Helmert model (2.29) and (2.30). Note that $\varepsilon_1 = -R_1$, $\varepsilon_2 = -R_2$, $\varepsilon_3 = -R_3$ (after [2.62, 65, 67])

From	To	$T_1\|\dot{T}_1$ (cm) (cm/y)	$T_2\|\dot{T}_2$ (cm) (cm/y)	$T_3\|\dot{T}_3$ (cm) (cm/y)	$\varepsilon_1\|\dot{\varepsilon}_1$ (0.001″) (0.001″/y)	$\varepsilon_2\|\dot{\varepsilon}_2$ (0.001″) (0.001″/y)	$\varepsilon_3\|\dot{\varepsilon}_3$ (0.001″) (0.001″/y)	$D\|\dot{D}$ (10^{-8}) (10^{-8}/y)	t_0
WGS72	ITRF90	−6.0	+51.7	+472.3	+18.3	−0.3	−547.0	+23.1	1984
WGS84[a]	ITRF90	−6.0	+51.7	+22.3	+18.3	−0.3	+7.0	+1.1	1984
PZ-90	PZ-90.02	−107	−3	+2	0	0	−130	−22	2002
PZ-90.02	WGS-84(1150)	−36	+8	+18	0	0	0	0	2002
PZ-90.11	ITRF2008	−0.3	−0.1	0.0	+0.019	−0.042	+0.002	0.0	2010
ITRF96	NAD83(CORS96)	+99.1	−190.7	−51.3	+25.8	+9.7	+11.7	0.0	1997
		0.0	0.0	0.0	+0.053	−0.742	−0.032	0.0	
ITRF97	NAD83(CORS96)	+98.9	−190.7	−50.3	+25.9	+9.4	+11.6	−0.09	1997
		+0.07	−0.01	+0.19	+0.067	−0.757	−0.031	−0.02	
ITRF2000	NAD83(CORS96)	+99.6	−190.1	−52.2	+25.9	+9.4	+11.6	+0.06	1997
		+0.07	−0.07	+0.05	+0.067	−0.757	−0.051	−0.02	

[a] original realization; for more recent realizations, see text.

according to the NNR-NUVEL1A model [2.54] by the rates

$$\begin{aligned}
\Omega_x &= +0.000258 \cdot 10^{-6}\,\mathrm{rad/y} &&= +0.053\,\mathrm{mas/y}\\
\Omega_y &= -0.003599 \cdot 10^{-6}\,\mathrm{rad/y} &&= -0.742\,\mathrm{mas/y}\\
\Omega_z &= -0.000153 \cdot 10^{-6}\,\mathrm{rad/y} &&= -0.032\,\mathrm{mas/y}
\end{aligned} \tag{2.34}$$

which explain the rotation parameter rates between NAD83 and ITRF in Table 2.3.

Coordinates of a control point in any particular frame are listed in terms of the Cartesian vector $\boldsymbol{x}_0$ and a velocity $\dot{\boldsymbol{x}}_0$, both at a given epoch t_0 so that at any other epoch the coordinates within that frame are

$$\boldsymbol{x}(t) = \boldsymbol{x}_0 + \boldsymbol{v}_0 (t - t_0)\,. \tag{2.35}$$

Transformation between frames and epochs requires consideration of both the point velocity within a frame and the velocity of the transformation parameters. Thus,

$$\boldsymbol{x}_{\text{from}}(t_0) \xrightarrow{\beta_0} \boldsymbol{x}_{\text{to}}(t_0) \xrightarrow{\dot{\boldsymbol{x}}_0} \boldsymbol{x}_{\text{to}}(t)\,, \tag{2.36}$$

or, also,

$$\boldsymbol{x}_{\text{from}}(t_0) \xrightarrow{\dot{\boldsymbol{x}}_{\text{from}}(t_0)} \boldsymbol{x}_{\text{from}}(t) \xrightarrow{\beta(t)} \boldsymbol{x}_{\text{to}}(t)\,. \tag{2.37}$$

Transformations (2.36) and (2.37) are equivalent if the point and frame velocities are related according to

$$\dot{\boldsymbol{x}}_{\text{to}} = \dot{\boldsymbol{x}}_{\text{from}} + \dot{\boldsymbol{T}} + \dot{\mathbf{D}}\boldsymbol{x}_{\text{from}} + \dot{\boldsymbol{\Omega}}\boldsymbol{x}_{\text{from}}\,, \tag{2.38}$$

where

$$\boldsymbol{\Omega} = \begin{pmatrix} 0 & -R_3 & +R_2 \\ +R_3 & 0 & -R_1 \\ -R_2 & +R_1 & 0 \end{pmatrix}, \tag{2.39}$$

which is the time derivative (neglecting second and higher order terms) of (2.29).

For most points within a regional frame, such as NAD83, the within-frame velocity of a point is small compared to the velocity of that same point in the ITRF, since, in this example, most of the velocity within the ITRF is due to the motion of the North American plate, and the NAD83 rides along with that plate. However, points on another plate within the NAD83 frame, such as points on the West Coast that are on the Pacific Plate, experience significant motion within the frame.

2.3.5 Earth Tides

Because the Earth is not a rigid body, the coordinates of points on its surface change in time in response to forces that deform its crust. The largest of these is due to the gravitational attractions of the Sun and Moon, which not only create the familiar periodic motion of the ocean tides, but also deform any point on (or below) the elastic Earth. The resulting periodic motion is called the *Earth tide* or *body tide*. Furthermore, because of the ocean tides, there is a secondary loading effect that deforms the crust especially at points near coastal areas. These tidal deformations are part of the corrections $\Delta\boldsymbol{x}_i(t)$ in (2.31).

In addition to the tide-induced corrections, there are other environmental effects, such as subsidence or uplift due to natural geophysical effects (earthquakes, post-glacial rebound) or anthropogenic activities (subsurface mineral and water extraction), and due to local hydrological effects (seasonal, secular, and episodic changes). These are site specific and dependent on local models.

The starting point for computing the tidal effect is the *tidal potential*, which accounts for the relative gravitational attraction of the Sun and Moon (other bodies have negligible effect). It is defined as the residual potential after removing the potential associated with the gravitational acceleration that is constant at all material points of the Earth. Assuming that the gravitational effect of a celestial body, B (e.g., the Sun, $\odot$, or Moon, $☾$), may be approximated as that of a point mass at location, (r_B, ϕ_B, λ_B), in the terrestrial reference system, the principal tidal potential at (r, ϕ, λ) and time t is given by [2.2, p. 132]

$$V^{(B)}(r,\phi,\lambda,t) = \frac{GM_B}{5r_B}\left(\frac{r}{r_B}\right)^2 \times \sum_{m=0}^{2} \overline{P}_{2,m}(\sin\phi)\,\overline{P}_{2,m}(\sin\phi_B)\cos(mt_B)\,, \tag{2.40}$$

where G is Newton's gravitational constant, M_B is the mass of the body, $\bar{P}_{2,m}$ is a second-degree, m-th order, fully normalized, associated Legendre function [2.42] and

$$t_B = t_\Upsilon^G + \lambda - \alpha_B \tag{2.41}$$

is the hour angle of the body, combining λ, the Greenwich sidereal time, t_Υ^G, and the right ascension, $\alpha_B = t_\Upsilon^G + \lambda_B$, of the body (Fig. 2.16). The coordinates, r_B, ϕ_B, α_B, and t_Υ^G are functions of time describing both the orbit of the body around the Earth and Earth rotation.

Equation (2.40) separates the long-period tides ($m = 0$) that have annual, semiannual, monthly, and fortnightly periods due to the orbital motion of the Earth and Moon, and the diurnal ($m = 1$) and semidiurnal ($m = 2$) tides due to Earth's rotation. In fact, (2.40) is an approximation that includes only the second-degree harmonics of the potential. Including third-degree harmonics, having the much smaller factor, $(r/r_B)^3$, and Legendre functions, $\bar{P}_{3,m}$, $m = 0, 1, 2, 3$, would introduce terdiurnal periods.

The tidal potential includes a permanent tide potential that is the average over time. Only the $m = 0$ term contributes and is calculated by averaging $\phi_B(t)$ over one orbit assuming r_B is constant [2.69],

$$V_{\text{perm}}^{(B)}(r,\phi) = \frac{3}{8}\frac{GM_B r^2}{r_B^2}\left(3\sin^2\phi - 1\right)\cdot\left(\sin^2\varepsilon - \frac{2}{3}\right), \tag{2.42}$$

where ε is the obliquity of the ecliptic (Sect. 2.4). Since the potential is a scalar function, the law of superposition says that the tidal potential due to all bodies is the sum of the individual tidal potentials; thus, $V = V^{☾} + V^{\odot}$.

The tidal deformation of points on the Earth derives heuristically from the elasticity of the Earth and *Hooke's law*, which states that a displacement of the end of an elastic spring (the Earth's surface in this case) is linearly proportional to an applied force (the gravitational pull by the body). The gravitational pull (per unit mass) is the gradient of the potential; and, as a vector it creates a three-dimensional deformation in the radial and locally horizontal directions (Fig. 2.7),

$$\begin{pmatrix} \Delta u \\ \Delta v \\ \Delta w \end{pmatrix} = \begin{pmatrix} \ell_2 \dfrac{a}{g_0} \dfrac{\partial V}{r \cos\phi \, \partial\lambda} \\ \ell_2 \dfrac{a}{g_0} \dfrac{\partial V}{r \partial\phi} \\ \dfrac{\mathrm{h}_2}{2} \dfrac{a}{g_0} \dfrac{\partial V}{\partial r} \end{pmatrix}, \tag{2.43}$$

where Earth's equatorial radius, a, and an average value of Earth's gravity, g_0, are introduced so that the *spring constants*, h_2, ℓ_2, are dimensionless (the subscript refers to the second-degree model of the tidal potential). Indeed, h_2 was postulated by A.E.H. Love in 1909 and has become known as a *Love number*. The factor of 2 is included here since Love originally assumed simple proportionality to the tidal potential. In fact, for points on a spherical Earth, $\partial V/\partial r = 2V/a$; see also [2.70] for a definition in terms of vector spherical harmonics that is adopted by the IERS. Likewise, ℓ_2 is called a *Shida number*, although both are now generically called Love numbers.

The displacements given by (2.43) include a component due to the permanent tide, (2.42); but, such a displacement is time invariant and cannot be observed. Although the IAG in 1984 recommended that station coordinates *not* be corrected for the permanent tidal deformation, the continuing practice is to apply the full tidal effect, thus placing the coordinates in a *tide-free system*, rather than the recommended *mean-tide system*, which only has time-varying components removed [2.6, p. 108].

Nominal values for the Love numbers are [2.6]

$$\mathrm{h}_2 = 0.61 \quad \text{and} \quad \ell_2 = 0.085\,, \tag{2.44}$$

which yield, with the corresponding astronomical constants for the Moon and Sun, a permanent deformation at the equator of $\Delta w_{☾}^{(0)} = 5.5\,\mathrm{cm}$ and $\Delta w_{\odot}^{(0)} = 2.5\,\mathrm{cm}$. The diurnal variations with respect to these mean values and the simple model above amount to less than 20 cm for the Moon and less than 10 cm for the Sun.

The Love numbers depend strongly on the density and elastic properties of the Earth, including its liquid core, and to a lesser extent on its ellipticity and changes in Earth orientation (nutation and polar motion). In particular, the resonance with the nearly diurnal free wobble (free core nutation, Sect. 2.5.3) is significant and illustrates that the Love numbers are also frequency dependent. The simple model has been extended with various levels of sophistication to account for the deformations observed with VLBI; see [2.70–72], and references therein, and [2.6] that summarizes the recommended formulas.

The secondary effect on station positions, due to ocean loading, depends on the ocean tide model and is computed using a convolution of ocean tide height with a Green's function [2.73]. The effect can be several percent of the body tide effect within continents and several 10% near the coast [2.30]. Another source of variable loading comes from the atmospheric tides resulting from the diurnal heating by the Sun. These mm-to-cm effects can be computed from corresponding atmospheric tidal models based on worldwide barometric data.

The centrifugal acceleration associated with Earth's rotation changes at a point with changes in the direction of the rotation axis with respect to the crust (and thus the terrestrial reference system). This implies a further deformation for an elastic Earth with the periods of polar motion (Sect. 2.5.3). It is called the *pole tide* although the source is not an external gravitational field. The centrifugal acceleration, $\boldsymbol{a}_c = \nabla V_c$, may be associated with a centrifugal potential, V_c, whose residual relative to $V_c^{(0)} = 0.5\omega_{\oplus}^2 \left(x^2 + y^2\right)$, is shown by [2.71] to be, in first-order approximation

$$\delta V_c = -\frac{\omega_{\oplus}^2}{2} r^2 \sin 2\phi \left(x_\mathrm{p} \cos\lambda - y_\mathrm{p} \sin\lambda\right), \tag{2.45}$$

where $x_\mathrm{p}, y_\mathrm{p}$ are the coordinates of the pole in the TRS (Sect. 2.5.3), measured in radians. This has the same form as the second-degree tidal potential (2.42) due to an extraterrestrial body; and, the corresponding crustal deformation is given by (2.43). Since $\left|x_\mathrm{p}\right|, \left|y_\mathrm{p}\right| \approx 0.2''$ relative to the current mean position, the vertical variation is of the order of 0.6 cm. The effect of ocean loading due to the pole tide, again, is site and ocean-basin model dependent and at the level of a millimeter [2.6, Chap. 7].

2.4 Celestial Reference System

Throughout history and today the ultimate reference system for positioning and navigation on and near the Earth, as well as within our solar system is an astronomic system. Its modern manifestation is the *celestial reference system* (CRS). By definition, it is an *inertial* system, which means that it is in free fall in the gravitational field of the universe and does not rotate. It is a system in which the laws of physics in the context of the theory of general relativity hold without requiring corrections for rotations. For geodetic purposes the CRS serves as the primal reference for positioning since it has no dynamics. Conversely, it is the system with respect to which we study the dynamics of the Earth as a rotating body. And, finally, it serves, of course, also as a reference system for astrometry.

The *celestial reference frame* (CRF) is the realization of the CRS based on a set of coordinates of objects on the celestial sphere. For this purpose the origin of the celestial sphere, and thus the CRS, is defined to be the *barycenter* of the solar system, which is the center of mass, as realized by the orbits of the planets. When appropriate or necessary, one also makes the distinction between the CRS and the *geocentric celestial reference system* (GCRS).

The origins, or zero points, of the celestial coordinates, declination and right ascension, have changed definition with a fundamental redefinition of the CRS in 1998. Prior to this time, the definition of the celestial reference system was tied directly to the dynamics of the Earth, whereas, today it is defined almost completely independent of the Earth, although the difference in realizations is defined to be minimal for the sake of continuity. The traditional system refers to two natural directions, the mean direction of Earth's spin axis, or the *north celestial pole* (NCP), and the direction of the *north ecliptic pole* (NEP), which is perpendicular to the mean ecliptic plane defined by Earth's orbit around the Sun (Fig. 2.14).

A point where the ecliptic crosses the celestial equator on the celestial sphere is called an equinox. At the *vernal equinox*, Υ, the Sun crosses the celestial equator from south to north as viewed from the Earth. It is the point on the Earth's orbit when Spring starts in the Northern Hemisphere. The angle between the celestial equator and the ecliptic is the *obliquity of the ecliptic*, approximately $\varepsilon = 23.44°$.

The direction of the vernal equinox defines the traditional origin for right ascension and the celestial equator is the origin for declination, as shown in Fig. 2.15. The system of celestial coordinates is also known as the *equatorial right ascension system*. The first and third axes of this system are, respectively, the directions of the vernal equinox and the NCP, which are perpendicular since the vernal equinox lies in the equatorial plane. The second axis is perpendicular to the other two axes so as to form a right-handed system. The intersection of the celestial sphere with the plane that contains both the third axis and a celestial object is called the *hour circle* of the object (Fig. 2.16). The right ascension system is the basis for the celestial reference system, where one must further fix the axes since both the vernal equinox and the NCP are dynamic directions that vary in time due to gravitational effects on Earth's rotational direction and its orbit.

The relationship between the right ascension and longitude on the Earth is illustrated in Fig. 2.16 under the assumption that the terrestrial pole and the NCP have the same direction (Sect. 2.5.1). The name, hour circle, refers to the convention that the right ascension of an object is also given in terms of a sidereal time interval (Sect. 2.1.3), where 15° of right ascension is equivalent to 1 h of sidereal time.

In order to define a reference system, it was necessary to establish the theory of motion of the NCP and the equinox, called the theory of nutation and precession (Sect. 2.5). Moreover, the realization of the reference system was stamped with an epoch for which it was valid; it was typical to determine a new realization every 25 years to reflect the dynamics of the reference system, as well as any updates in the theories

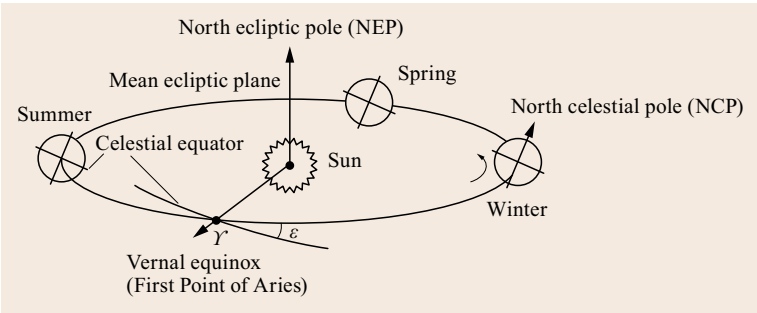

Fig. 2.14 Mean ecliptic plane (seasons are for the Northern Hemisphere). and natural directions for the celestial reference system

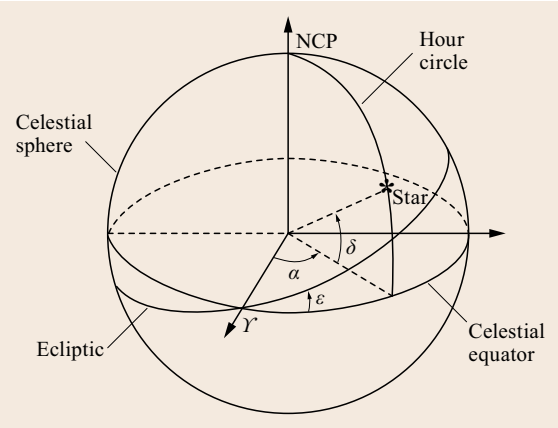

Fig. 2.15 Celestial coordinates, α, δ, in the equatorial right ascension system

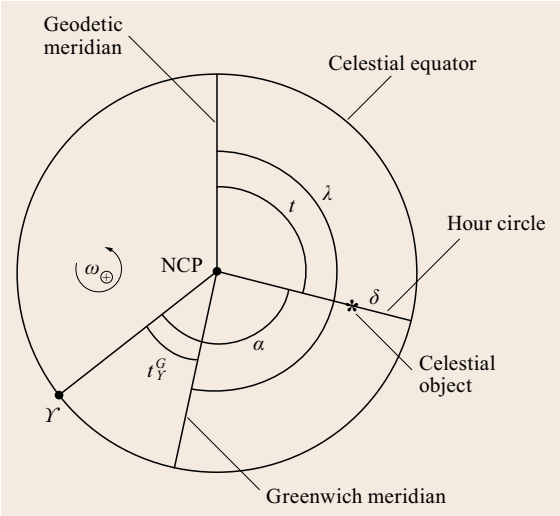

Fig. 2.16 Relationship between right ascension and longitude (idealized without polar motion). The meridian of a terrestrial point and the Greenwich meridian rotate relative to the vernal equinox due to Earth's rotation rate, $\omega_{\oplus}$. The hour angle, t_{Υ}^{G}, is also the Greenwich sidereal time

of motion [2.5, p. 167]. The last such realization was the FK5 (Fundamental Catalog No. 5) of stars referring to the best computed equinox and NCP for the epoch, J2000. The origins of right ascension and declination were determined indirectly from an adjustment of observed coordinates of celestial objects and their proper motions (in other words, the equinox is not observed directly).

The change in definition of the CRS adopted by the International Astronomical Union (IAU) in the 1990s was enabled by the then established history of very accurate observations of quasars (quasi-stellar radio sources) using the technique of Very Long Baseline Interferometry (VLBI, [2.39, Chap. 11.1]). Since these beacons are at such great distances that no proper motion can be detected, that is, they have no perceptible rotation on the celestial sphere, they may be used to define an inertial system.

This new definition of the CRS represents a change as fundamental as that which transferred the origin of the regional terrestrial reference system (i. e., the horizontal geodetic datum) from a monument on Earth's surface to the geocenter. By relying strictly on geometrically defined points on the celestial sphere, the definition of the CRS has changed from a *dynamic* system to a *kinematic* (or geometrical) system. The axes of the celestial reference system are still (close to) the NCP and vernal equinox, but are not defined dynamically in connection with Earth's motion. Rather they are tied to the defining set of quasars whose coordinates are given with respect to these axes. Moreover, there is no need to define an epoch of reference, because (presumably) these directions will never change in inertial space (at least in the foreseeable future of mankind).

The IERS officially created the *International Celestial Reference System* (ICRS) starting in 1998 based on 212 defining sources, which then also constitute the realization of the system, the *International Celestial Reference Frame* (ICRF). An additional 396 *candidate* or other less well observed sources were used as additional ties to the reference frame. The origin of the ICRS is defined to be the center of mass of the solar system (*barycentric* system) and is realized by observations of planets and other bodies in the solar system (such as the Jet Propulsion Laboratory (JPL) development ephemerides) in the framework of the theory of general relativity. These dynamical planetary ephemerides are aligned with the ICRF to high accuracy [2.6, Chap. 3].

By Recommendation VII of the 1991 IAU General Assembly, the NCP and equinox of the ICRS are supposed to be close to the mean dynamical pole and equinox of J2000.0. Furthermore, the adopted pole and equinox for ICRS should be consistent with the directions realized for FK5. Specifically, the origin of right ascension for FK5 was originally defined on the basis of the mean right ascension of 23 radio sources from various catalogs, with the right ascension of one particular source fixed to its FK4 value, transformed to J2000.0. Similarly, the FK5 pole was based on its J2000.0 direction defined using the 1976 precession and 1980 nutation series (Sect. 2.5). The FK5 directions are estimated to be accurate to ± 50 mas (milli-arcsec) for the pole and ± 80 mas for the equinox; and, it is now known, from improved observations and dynamical models, that the ICRS pole

and equinox are close to the mean dynamical equinox and pole of J2000.0, well within these tolerances. The precise transformation to a dynamical system is a *frame bias* that is included in the modern formulations of the transformations between the celestial and terrestrial reference frames (Sect. 2.5). This bias is well determined and of the order of 10 mas [2.6, 74].

As the VLBI measurements of the quasars improve, the orientation of the ICRF will be adjusted with the constraint that it has no net rotation with respect to previous realizations (analogous to the ITRF). The original realization is designated ICRF1; and, it was extended in 1999 and again in 2002 with additional objects observed by VLBI, totaling 667 and 717, respectively. The next significant realization, designated ICRF2, was constructed in 2009, where now 295 quasars define the system (being more stable and better distributed in the sky than for ICRF1), and which also includes 3119 secondary extragalactic sources.

Aside from VLBI, the principal realization of the ICRS is through the Hipparcos catalog, based on recent observations of some 120 000 well-defined stars using the Hipparcos (High Precision Parallax Collecting Satellite), optical, orbiting telescope. This catalog is tied to the ICRF with an accuracy of about 0.6 mas in each axis. Additional catalogs for up to 100 million stars are described by [2.6].

2.5 Transformations Between ICRF and ITRF

The transformation from the CRF to the terrestrial reference frame requires an understanding of the dynamics of Earth rotation and its orbital motion, as well as the effects of observing celestial objects on a moving and rotating body such as the Earth. Even though the new definition of the celestial reference system (Sect. 2.4) no longer relies on models for the dynamics of the Earth's pole and the vernal equinox, but because the terrestrial system is fixed to the Earth, any transformation between celestial and terrestrial frames still does depend explicitly on these dynamics.

The description of the transformation, comprising *Earth orientation parameters*, has also changed with the adoption of the new system definition. Here, both the traditional description and the modern transformation are treated, where the traditional one is perhaps a bit more accessible in terms of physical intuition, whereas, the latter tends to hide these concepts. Furthermore, the new approach implements certain nuances necessary for an unambiguous definition of Earth rotation. Thus, the following starts with the traditional approach and evolves into the modern transformation formulas.

The theoretical description of Earth's *dynamics* in inertial space requires a system of time, and dynamic time, being theoretically the most uniform in scale (Sect. 2.1) is the natural choice. Because many of the dynamics vary on scales of years or longer, the time variable, τ, is expressed typically as a (unit-less) fraction of a Julian century relative to a fixed epoch

$$\tau = \frac{t - t_0}{36\,525}\,, \tag{2.46}$$

where $t_0 = 2451545.0$ is the Julian day number for J2000.0 and t is the Julian day number of the epoch of date.

2.5.1 Orientation of the Earth in Space

The gravitational interaction of the Earth with the other bodies of the solar system, including primarily the Moon and the Sun, but also the planets, cause Earth's orbital motion to deviate from the simple Keplerian motion of two point masses in space. Also, because the Earth is not a perfect homogeneous sphere, its rotation is affected likewise by the gravitational action of the bodies in the solar system. If there were no other planets (only the Earth/Moon system) then the orbit of the Earth/Moon system around the Sun would be essentially a plane fixed in space. This plane defines the ecliptic (Sect. 2.4). But the gravitational forces of the planets cause this ecliptic plane to behave in a dynamic way, called *planetary precession*.

If the obliquity of the ecliptic were zero (or the Earth were not flattened at its poles), then there would be no gravitational torques due to the Sun, Moon, and planets acting on the Earth's bulging equator. But since $\varepsilon \neq 0$ and $f \neq 0$, these celestial bodies (primarily, the Sun and Moon) do cause a precession of the equator and, hence, the pole, that is known as *luni-solar precession* and *nutation*, depending on the period of the motion [2.75]. That is, the equatorial bulge of the Earth and its tilt with respect to the ecliptic allow the Earth to be torqued by the gravitational forces of the Sun, Moon, and planets, since they all lie approximately on the ecliptic plane. Planetary precession together with luni-solar precession is known as *general precession*.

The complex dynamics of the precession and nutation is a superposition of many periodic motions originating from the myriad of periods associated with the orbital dynamics of the corresponding bodies. Conventionally, the period of 18.6 years associated with

the longest lunar cycle separates nutation from precession, where the latter can be described virtually as a secular motion of the pole and equinox owing to their fundamental respective periods of about 25 800 and 28 100 years. The periods of nutation depend primarily on the orbital motion of the Moon relative to the orbital motion of the Earth. The most recent models for nutation also contain short-periodic effects due to the relative motions of the planets. In terms of transformations, precession has been viewed as an accumulation of *mean* motion over a time interval, whereas, nutation is thought of as the correction, or residual, that transforms from the mean to the true location of the pole and equinox at a particular instant in time.

The theory for determining the motions of the coordinate reference directions was developed by Simon Newcomb at the turn of the twentieth century. Its basis lies in celestial mechanics and involves the n-body problem for planetary motion, for which no analytical solution exists. Instead, iterative, numerical procedures have been developed and formulated [2.76].

Precession

Planetary precession may be described by two angles, π_A and Π_A, where the subscript, A, refers to the *accumulated* angle from some fixed epoch, t_0, to some other epoch, t. Figure 2.17 shows the geometry of the motion of the ecliptic due to planetary precession from t_0 to t. The pictured ecliptics and equator are fictitious in the sense that they are affected only by precession, but not nutation, and as such are called *mean ecliptic* and *mean equator*. The angle, π_A, is the angle between the mean ecliptics at t_0 to t; while, Π_A is the ecliptic longitude of the point, M, on the celestial sphere, which identifies the axis of rotation of the ecliptic due to planetary precession. The vernal equinox at t_0 is denoted by Υ_0. Expressions for π_A and Π_A are truncated time series based on the celestial dynamics of the planets.

The *luni-solar precession*, on the other hand, also depends on the geophysical parameters of the Earth. Due to the more complicated nature of the Earth's shape and internal constitution, no analytic formula based on theory has been used for this part of the precession. Instead, Newcomb gave an empirical parameter, (now) called *Newcomb's precessional constant*, based on observed rates of precession. In fact, this *constant* rate is not strictly constant, as it depends slightly on time through a general relativistic term called the *geodesic precession* [2.77]. Newcomb's precessional constant depends on Earth's moments of inertia and enters in the dynamical equations of motion for the celestial equator due to the gravitational torques of the Sun and Moon.

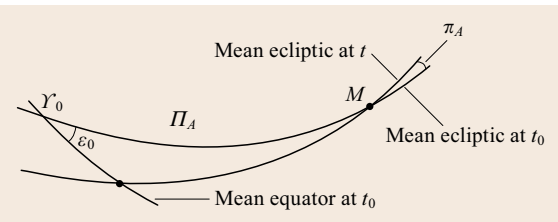

Fig. 2.17 Planetary precession

Figure 2.18 shows the accumulated angles of planetary and luni-solar precession near the vernal equinox. The precession angles, ψ_A and χ_A, respectively, describe the motion of the mean vernal equinox along the mean ecliptic (luni-solar precession) and along the mean equator (planetary precession).

Due to their virtually secular variation over the near term (few thousands of years), the planetary and luni-solar precessional angles are expressed as polynomials in time, formulated with a certain set of adopted constants and a dynamical theory. The developments of Newcomb and his contemporaries was reformulated and extended in precision by [2.77] based on constants adopted by the IAU. This was further extended in precision and updated in 2000 and again in 2006 by the IAU based on the works of [2.58, 78]. The resulting model, designated the IAU 2006 precession, includes, for example, expressions

$$\begin{aligned}\psi_A &= 5038.481507''\tau - 1.0790069''\tau^2 \\ &\quad - 0.00114045''\tau^3 + \cdots \\ \chi_A &= 10.556403''\tau - 2.3814292''\tau^2 \\ &\quad - 0.00121197''\tau^3 + \cdots ,\end{aligned} \tag{2.47}$$

for the angles ψ_A and χ_A, where τ is given by (2.46) and where fourth- and fifth-order terms are omitted here for brevity. The linear parts then give the instantaneous rates of precession at t_0. The rate of luni-solar precession of the vernal equinox along the mean ecliptic is

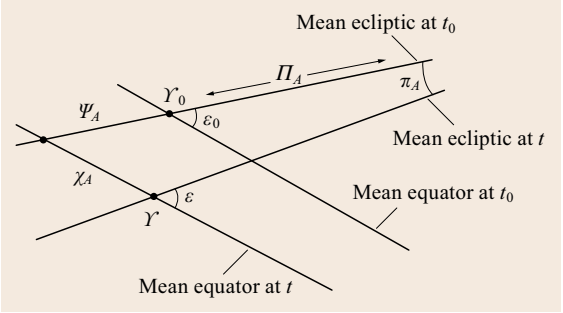

Fig. 2.18 General precession of the vernal equinox. Planetary precession along the mean equator is indicated by the angle, χ_A, and ψ_A denotes the luni-solar precession along the mean ecliptic (not to scale)

approximately

$$\frac{\mathrm{d}}{\mathrm{d}\tau}\psi_A\bigg|_{\tau=0} \approx 50.4''/\mathrm{y}\,, \tag{2.48}$$

and the planetary precession of Υ along the mean equator is approximately

$$\frac{\mathrm{d}}{\mathrm{d}\tau}\chi_A\bigg|_{\tau=0} \approx 0.106''/\mathrm{y}\,. \tag{2.49}$$

Combined the vernal equinox has a rate on the mean equator of about $(50.4''/\mathrm{y}\cdot\cos\varepsilon_0) - 0.106''/\mathrm{y} = 46.1''/\mathrm{y}$, which prompted the recently revised definition of Earth rotation angle that removes this from the defined origin for right ascension in the instantaneous celestial coordinate system and thus indicates pure Earth rotation rate (Sect. 2.1.3).

Luni-solar precession is by far the largest component of general precession and causes the Earth's spin axis to precess with respect to the celestial sphere and around the ecliptic pole with a period of about 25 800 years. Expressions similar to (2.47) for other angles (e.g., the obliquity of the ecliptic, ε) are given by [2.78].

One way to determine the changes in celestial coordinates due to the effect of general precession of the coordinate frame is with the use of the precessional elements, ζ_A, z_A, θ_A, defined in Fig. 2.19. Let the coordinates of a point on the celestial sphere be α_0, δ_0 at t_0, and due to precession of the frame, they become α_m, δ_m at epoch, t. In terms of unit vectors, define these points

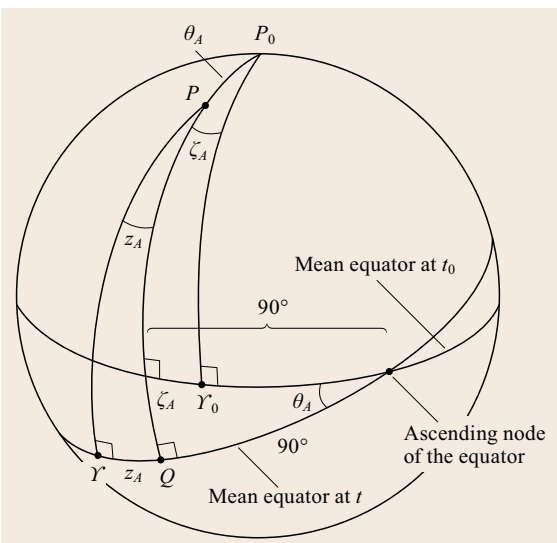

Fig. 2.19 Traditional precessional elements, ζ_A, z_A, θ_A, for the coordinate frame at epoch, t, relative to the frame at t_0

as

$$\boldsymbol{r}_0 = \begin{pmatrix} \cos\alpha_0\cos\delta_0 \\ \sin\alpha_0\cos\delta_0 \\ \sin\delta_0 \end{pmatrix} \tag{2.50}$$

and $\boldsymbol{r}_m$, analogously. Then, the transformation between the two frames is achieved by the rotations

$$\begin{aligned} \boldsymbol{r}_m &= \mathbf{R}_3(-z_A)\mathbf{R}_2(+\theta_A)\mathbf{R}_3(-\zeta_A)\,\boldsymbol{r}_0 \\ &= \mathbf{P}\boldsymbol{r}_0 \end{aligned} \tag{2.51}$$

where it is noted that the great circle arc, $\widehat{\mathrm{P_0PQ}}$, intersects both mean equators of t_0 and of t at right angles because it is an hour circle with respect to both poles, P_0 and P. $\mathbf{R}_j\left(\alpha_j\right)$ denotes the usual orthogonal rotation matrix for a rotation by the angle, α_j, about the j-th axis of a right-handed Cartesian coordinate system (Table 2.4). $\mathbf{P}$ is called the *precession transformation matrix*.

The precessional elements for the IAU 2006 model [2.78, 81] are given by

$$\begin{aligned} \zeta_A &= 2.650545'' + 2306.083227''\tau \\ &\quad + 0.2988499''\tau^2 + 0.01801828''\tau^3 \\ &\quad - 0.5971''\cdot 10^{-6}\tau^4 - 3.173''\cdot 10^{-7}\tau^5 \\ z_A &= -2.6505453'' + 2306.0771813''\tau \\ &\quad + 1.09273483''\tau^2 + 0.018268373''\tau^3 \\ &\quad - 28.596''\cdot 10^{-6}\tau^4 - 2.904''\cdot 10^{-7}\tau^5 \\ \theta_A &= 2004.191903''\tau - 0.4294934''\tau^2 \\ &\quad - 0.041822''\tau^3 - 7.089''\cdot 10^{-6}\tau^4 \\ &\quad - 1.274''\cdot 10^{-7}\tau^5\,, \end{aligned} \tag{2.52}$$

where, however, these expressions do not include the frame bias introduced with the change in celestial reference system definition (Sect. 2.4).

Nutation

The nutations, also called *astronomic nutations*, describe the dynamics over the shorter periods, and, indeed, they are modeled as a series of sines and cosines. As a correction to the mean frame at the epoch of date, t, the transformation for nutation yields coordinates in the *true* or *instantaneous* frame. This true frame is called the intermediate frame in transformations between the celestial and terrestrial frames and is discussed in more detail in Sect. 2.5.4.

Since the nutations are primarily due to the luni-solar attractions, they are modeled firstly in terms of the ecliptic coordinates of the Sun and Moon. Traditionally, the nutations are expressed by two angles, $\Delta\varepsilon$ and $\Delta\psi$, that, respectively, describe the change (from mean to

Table 2.4 Elementary rotation matrices. Multiplication of a coordinate vector referred to a frame $\mathcal{R}_{\text{from}}$ by matrix $\mathbf{R}_i$ provides the coordinates of the same vector in a frame $\mathcal{R}_{\text{to}}$, which is obtained from $\mathcal{R}_{\text{from}}$ by a right-handed rotation by angle α about the i-th axis (after [2.79, 80])

Rotation about x-axis:	Rotation about y-axis:	Rotation about z-axis:
$\mathbf{R}_1(\alpha) = \begin{pmatrix} 1 & 0 & 0 \\ 0 & +\cos\alpha & +\sin\alpha \\ 0 & -\sin\alpha & +\cos\alpha \end{pmatrix}$	$\mathbf{R}_2(\alpha) = \begin{pmatrix} +\cos\alpha & 0 & -\sin\alpha \\ 0 & 1 & 0 \\ +\sin\alpha & 0 & +\cos\alpha \end{pmatrix}$	$\mathbf{R}_3(\alpha) = \begin{pmatrix} +\cos\alpha & +\sin\alpha & 0 \\ -\sin\alpha & +\cos\alpha & 0 \\ 0 & 0 & 1 \end{pmatrix}$

true) in the tilt of the equator with respect to the mean ecliptic, and the change (again, from mean to true) of the equinox along the mean ecliptic (Fig. 2.20). There is no need to transform from the mean to the true ecliptic since only the dynamics of the true equator are of interest. The true vernal equinox, Υ_T, is always defined to be on the mean ecliptic.

The *nutation in longitude*, $\Delta\psi$, is primarily caused by the ellipticities of the Earth's and Moon's orbits. The *nutation in obliquity*, $\Delta\varepsilon$, is mainly due to the Moon's orbital plane being out of the ecliptic (by about 5.145°). Models for the nutation angles are given in the form

$$\Delta\psi = \sum_{i=1}^{n} \left(a_i \sin A_i + a_i' \cos A_i\right)$$
$$\Delta\varepsilon = \sum_{i=1}^{n} \left(b_i \cos A_i + b_i' \sin A_i\right) , \qquad (2.53)$$

where each amplitude, a_i, a_i', b_i, b_i', is a linear function of τ and the angle

$$A_i = n_{\ell,i}\ell + n_{\ell',i}\ell' + n_{F,i}F + n_{D,i}D + n_{\Omega,i}\Omega , \qquad (2.54)$$

represents a linear combination of fundamental arguments (*Delaunay variables*, [2.82]) of the solar and lunar orbits:

- ℓ Mean anomaly of the Moon,
- ℓ' Mean anomaly of the Sun,
- F Mean longitude of the Moon minus the mean longitude of the Moon's ascending node,
- D Mean elongation of the Moon from the Sun,
- Ω Mean longitude of the ascending node of the Moon.

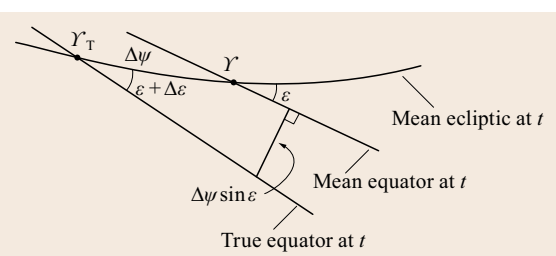

Fig. 2.20 Nutation elements, $\Delta\varepsilon$ and $\Delta\psi$

The corresponding arguments are introduced for the planetary orbits in an expanded theory. The integer multipliers, $n_{\ell,i}, \ldots, n_{\Omega,i}$, specify how these variables are combined in the argument, A_i.

The theory and series developed by [2.76] included $n = 69$ terms for $\Delta\psi$ and $n = 40$ terms for $\Delta\varepsilon$. The subsequent theory and series [2.83] adopted by the IAU in 1980, which included modifications for a nonrigid Earth model [2.71] had $n = 106$ terms. The IAU1980 nutation model was replaced in 2003 by the new nutation model of [2.58], designated IAU2000A (2000B is an abbreviated, less precise version). This model accounts for the mantle anelasticity, the effects of ocean tides, electromagnetic couplings between the mantle, the fluid outer core, and the solid inner core, as well as various nonlinear terms not previously considered.

A slight revision of the model due to the new IAU 2006 precession model is designated the IAU2000A$_{\text{R06}}$ nutation model, which has 1320 terms for $\Delta\psi$ and 1037 terms for $\Delta\varepsilon$ ([2.6] and [2.84, Tables 5.3a,b]). Table 2.5 summarizes the largest of the nutation amplitudes and associated variables and parameters according to this model. The corresponding expressions for the Delaunay variables as low-order polynomials in τ are also given in [2.6, p. 67]. The periods of the nutations may be computed from the linear coefficients of the resulting polynomial expressions for the angle, A_i. The high-index angles, A_i, also include the longitudes of the planets. The frame bias (Sect. 2.4) is already incorporated in Table 2.5.

Figure 2.21 depicts the motion of the pole due to the dominant luni-solar precession combined with the largest of the nutation terms. This diagram also defines the *nutational ellipse* that describes the extent of the true motion with respect to the mean motion. The semi-axis of this ellipse that is orthogonal to the mean motion is the principal term in the nutation in obliquity and is also known as the *constant of nutation*. The values for it and for the other semi-axis, given by $\Delta\psi \sin\varepsilon$ (Fig. 2.20), can be inferred from Table 2.5. The total motion of the pole on the celestial sphere is due to the superposition of the general precession and all the nutations.

The transformation at the epoch of date, t, from the mean frame to the true frame, referring to Fig. 2.20, is

Table 2.5 The dominant terms of the IAU2000A$_{R06}$ series for nutation in longitude and obliquity, referred to the mean ecliptic of date. τ, as defined in (2.46) denotes the number of Julian centuries since 1.5 Jan 2000. Note that the index i does not correspond to the order of the IAU $\Delta\varepsilon$ components.

i	Period (d)	a_i (10^{-6} ″)		b_i (10^{-6} ″)		$n_{\ell,i}$	$n_{\ell',i}$	$n_{F,i}$	$n_{D,i}$	$n_{\Omega,i}$
1	6798.4	−17 206 424.18	−17 418.82τ	+9 205 233.10	+883.03τ	0	0	0	0	+1
2	182.6	−1 317 091.22	−1369.60τ	+573 033.60	−458.70τ	0	0	+2	−2	+2
3	13.7	−227 641.81	+279.60τ	+97 846.10	+137.40τ	0	0	+2	0	+2
4	3399.2	+207 455.40	−69.80τ	−89 749.20	−29.10τ	0	0	0	0	+2
5	365.3	+147 587.70	+1181.70τ	+7387.10	−192.40τ	0	+1	0	0	0
6	27.6	+71 115.90	−87.20τ	−675.00	+35.80τ	+1	0	0	0	0
7	121.7	−51 682.10	−52.40τ	+22 438.60	−17.40τ	0	+1	+2	−2	+2
8	13.6	−38 730.20	+38.00τ	+20 073.00	+31.80τ	0	0	+2	0	+1
9	9.1	−30 146.40	+81.60τ	+12 902.60	+36.70τ	+1	0	+2	0	+2

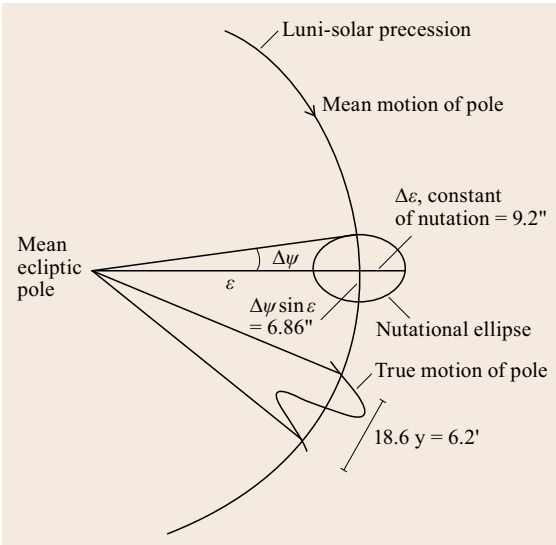

Fig. 2.21 Dominant components of the combined general precession and nutation of the pole on the celestial sphere

accomplished with the following rotations,

$$\begin{aligned} \boldsymbol{r} &= \mathbf{R}_1(-\varepsilon-\Delta\varepsilon)\mathbf{R}_3(-\Delta\psi)\mathbf{R}_1(\varepsilon)\,\boldsymbol{r}_m \\ &= \mathbf{N}\,\boldsymbol{r}_m \end{aligned} \tag{2.55}$$

where ε is the mean obliquity at epoch, t, and the true right ascension and declination are related to $\boldsymbol{r}$ as in (2.50).

The combined transformation due to precession and nutation from the epoch, t_0, to the current epoch, t, is given by the combination of equations (2.51) and (2.55),

$$\boldsymbol{r} = \mathbf{NP}\,\boldsymbol{r}_0\,. \tag{2.56}$$

The IAU 2006/2000A precession–nutation model is accurate to about 0.3 mas. For those seeking the highest accuracy and temporal resolution, small corrections (called *celestial pole offsets*) obtained from continuing VLBI observations, may be applied to the nutation series. For example, the most recent model does not contain the diurnal motion due to the free-core nutation (FCN) caused by the interaction of the mantle and the rotating fluid outer core ([2.75]; see also Sect. 2.5.3). The IERS publishes differential elements in longitude, $\delta\psi$, and obliquity, $\delta\varepsilon$, that can be added to the elements implied by the nutation series

$$\begin{aligned} \Delta\psi &= \Delta\psi\ (\text{model}) + \delta\psi \\ \Delta\varepsilon &= \Delta\varepsilon\ (\text{model}) + \delta\varepsilon\,. \end{aligned} \tag{2.57}$$

2.5.2 New Conventions

The new definition of the celestial reference system (CRS, Sect. 2.4) was prompted not only by the ability to realize the system geometrically with accurate VLBI observations, but also by a critical analysis of the system conventions for the origin of right ascension [2.85, 86]. Specifically, by avoiding a dynamical definition of the CRS axes, there is no particular reason to use the vernal equinox on the mean ecliptic as an origin of right ascensions, especially because even in the mean it is a dynamical point on the celestial sphere. That is, as an origin point it rotates about the NCP due to the precessional rotation of the ecliptic. This must then be corrected when considering the rotation of the Earth with respect to inertial space (Greenwich sidereal time, or the hour angle at Greenwich of the vernal equinox; Sect. 2.1.3).

In 2000, the IAU adopted a set of resolutions that precisely adhered to a new, more accurate, and simplified way of dealing with the transformation between the celestial and terrestrial reference systems. The IERS, in 2003, similarly adopted the new methods based on these resolutions [2.87]. These were reinforced with IAU resolutions in 2006 and adopted as part of the IERS Conventions 2010. The true NCP, previously also called the celestial ephemeris pole (CEP) with a resolution of

the IAU in 1979, now is called the celestial intermediate pole (CIP), thus identifying it as a transition between celestial and terrestrial reference frames. The new conventions also revised the origin for right ascension in this intermediate frame so as to eliminate residual rotations not associated with Earth rotation, while also ensuring continuity with the previously defined origin. These profoundly new definitions solidify the paradigm of *kinematics* (rather than dynamics) upon which the celestial reference system is based. In addition, the description of precession and nutation is now combined in a single transformation from t_0 to t.

Suppose that the instantaneous pole, P, on the celestial sphere coincides with the reference pole, P_0, at some fundamental epoch, t_0. At the epoch of date, t, the position of P then has celestial coordinates as shown in Fig. 2.22. These coordinates are the co-declination, d, and the right ascension, E, with respect to the reference origin, Σ_0. The true or instantaneous equator (the plane perpendicular to the axis through P) at time, t, intersects the reference equator (associated with P_0) at two nodes that are 180° apart. The hour circle of the node, N, is orthogonal to the great circle arc $\widehat{P_0P}$. Therefore, the right ascension of the ascending node of the equator is 90° plus the right ascension of the instantaneous pole, P. The origin for right ascension at the epoch of date, t, is defined kinematically under the condition that there is no rotation *rate* of the *instantaneous coordinate frame* about the pole due to precession and nutation. This is the concept of the *nonrotating origin* (NRO), which, as origin for right ascensions on the instantaneous equator, is now called the CIO; denoted as σ in Fig. 2.22).

Rather than successive transformations involving precessional elements and nutation angles, the transformation is more direct in terms of the coordinates, d and E. The additional parameter s defines the instantaneous origin of right ascension as an NRO (see below). Analogous to (2.51) and (2.55),

$$\begin{aligned} \boldsymbol{r} &= \mathbf{R}_3(-s)\mathbf{R}_3(-E)\mathbf{R}_2(d)\mathbf{R}_3(E)\,\boldsymbol{r}_0 \\ &= \mathbf{Q}^{\top}\boldsymbol{r}_0\,, \end{aligned} \tag{2.58}$$

which is easily derived by considering the successive rotations as the origin point transforms from the reference origin, Σ_0, to the instantaneous origin, σ (Fig. 2.22). Equation (2.58) not only replaces (2.56), but also incorporates the new conventions for defining the intermediate origin in right ascension (it is no longer the true vernal equinox). The IERS Conventions 2003 (and later) define the transformation matrix, $\mathbf{Q}$, as a rotation *from* the system of the instantaneous pole and origin *to* the reference system.

The total rotation rate of the pole, P, in inertial space is due to the rates in the coordinates, d, E, and in the

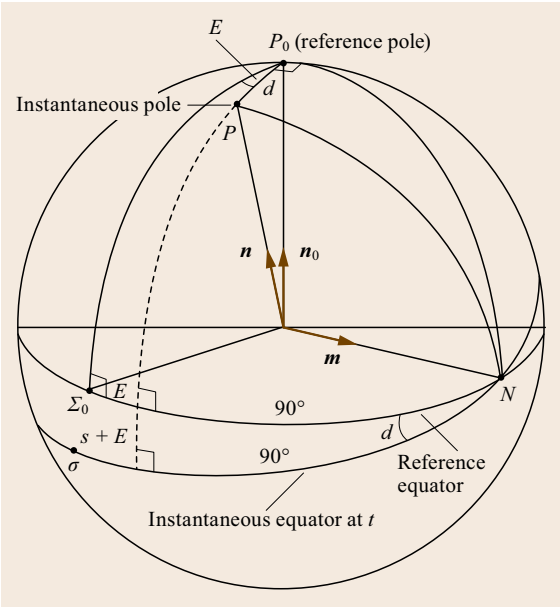

Fig. 2.22 Coordinates of the instantaneous pole in the celestial reference system

parameter, s. Defining three noncolinear unit vectors, $\boldsymbol{n}_0$, $\boldsymbol{m}$, $\boldsymbol{n}$, as shown in Fig. 2.22, the total rotation rate may be expressed as

$$\boldsymbol{\Theta} = \boldsymbol{n}_0\dot{E} + \boldsymbol{m}\dot{d} - \boldsymbol{n}\left(\dot{E} + \dot{s}\right), \tag{2.59}$$

where the dots denote time derivatives. Now, s is chosen so that the total rotation rate, $\boldsymbol{\Theta}$, has no component along $\boldsymbol{n}$. That is, s defines the origin point, σ, on the instantaneous equator that has no rotation rate about the corresponding polar axis (it is thus a nonrotating origin). This condition is formulated as $\boldsymbol{\Theta}\cdot\boldsymbol{n} = 0$, meaning that there is no component of the total rotation rate along the instantaneous polar axis. Since $\boldsymbol{n}\cdot\boldsymbol{m} = 0$ and $\boldsymbol{n}\cdot\boldsymbol{n}_0 = \cos d$, (2.59) implies that

$$\dot{s} = (\cos d - 1)\,\dot{E}\,. \tag{2.60}$$

Defining coordinates

$$\begin{pmatrix} X \\ Y \\ Z \end{pmatrix} = \begin{pmatrix} \sin d \cos E \\ \sin d \sin E \\ \cos d \end{pmatrix}, \tag{2.61}$$

it is easily shown that

$$\mathbf{Q} = \begin{pmatrix} 1 - aX^2 & -aXY & X \\ -aXY & 1 - aY^2 & Y \\ -X & -Y & 1 - a(X^2+Y^2) \end{pmatrix} \mathbf{R}_3(s) \tag{2.62}$$

where $a = 1/(1+\cos d)$. Furthermore, since

$$X\dot{Y} - Y\dot{X} = -\dot{E}\left(Z^2 - 1\right), \tag{2.63}$$

(2.60) integrates to

$$s = s_0 - \int_{t_0}^{t} \frac{X\dot{Y} - Y\dot{X}}{1+Z} \mathrm{d}t\,, \tag{2.64}$$

where $s_0 = s(t_0)$ is chosen so as to ensure continuity with the previous definition of the origin point at the epoch January 1, 2003.

Expressions for X and Y can be obtained directly from the precession and nutation equations [2.86]. For the latest IAU 2006/2000A precession–nutation models [2.6],

$$\begin{aligned} X = &-0.016617'' + 2004.191898''\tau \\ &- 0.4297829''\,\tau^2 - 0.19861834''\tau^3 \\ &- 0.000007578''\,\tau^4 - 0.0000059285''\tau^5 \\ &+ \sum_{i=1}^{n} \left(e_i \sin A_i + e_i' \cos A_i\right) \\ Y = &-0.006951'' - 0.025896''\,\tau \\ &- 22.4072747''\,\tau^2 + 0.00190059''\,\tau^3 \\ &+ 0.001112526''\,\tau^4 - 0.0000001358''\,\tau^5 \\ &+ \sum_{i=1}^{n} \left(f_i \sin A_i + f_i' \cos A_i\right), \end{aligned} \tag{2.65}$$

where τ is given by (2.46), the coefficients, e_i, e_i', f_i, f_i' are polynomials in τ, and the angles, A_i, are given by (2.54) including, for the higher indices, i, expressions for the longitudes of the planets (see Tables 5.2a,b in the electronic supplement [2.84] to the IERS Conventions 2010 [2.6]).

The corresponding series expression for the parameter s includes all terms larger than 0.5 µas (microarcsec), as well as the constant s_0

$$\begin{aligned} s = &-\frac{1}{2}XY + 94 + 3808.65\,\tau \\ &- 122.68\,\tau^2 - 72574.11\,\tau^3 \\ &+ \sum_k C_k \sin\alpha_k + \sum_k D_k \sin\beta_k \\ &+ \sum_k E_k \tau \cos\gamma_k + \sum_k F_k \tau^2 \sin\theta_k \ (\mu\mathrm{as})\,. \end{aligned} \tag{2.66}$$

The coefficients C_k, D_k, E_k, F_k and the arguments, α_k, β_k, γ_k, θ_k, are elaborated by [2.6, p. 59]. Values of s are less than 0.01″ (until the early 2030s) and can be ignored for transformations at that level of accuracy.

The transformation formulas (2.65) and (2.66) yield an accuracy of about $0.3 \cdot 10^{-3}$″ in the position of the pole and incorporate the frame bias described in Sect. 2.4.

2.5.3 Polar Motion

The previous sections describe Earth's orientation from the celestial perspective – how the direction of an axis, such as the spin axis, progresses in time on the celestial sphere due to precession and nutation. From the terrestrial view, however, the spin axis and various other axes associated with Earth's rotation and geometry also exhibit motion with respect to the Earth's crust due to the natural dynamics of the rotation. Euler's equations describe the motion of the principal (geometric) axes for a rigid body, but because the Earth is partially fluid and elastic, the motion of these axes is not accurately predictable.

The details of the theoretical and mathematical developments of the dynamics equations for elastic rotating bodies may be found in [2.37]. These dynamics are influenced both by the internal composition and fluid characteristics of the Earth (nonforced, or free motion) and external gravitational torques that deform the Earth (forced motion). For example, the free motion of the principal axis (also called *figure axis*) corresponding to Earth's polar axis of symmetry has a circular diurnal motion relative a mean fixed location (*mean Tisserand axis*) with radius of about 60 m. The spin and angular momentum axes, on the other hand, have an order of magnitude smaller motion due to their greater stability, or relative insensitivity to Earth's deformation.

The change in direction of an axis, such as the instantaneous spin axis, of the Earth with respect to the surface of the Earth is called *polar motion* (also *wobble*). The motion is described by local coordinates, x_p,y_p, with respect to the reference pole of the terrestrial reference system. Figure 2.23 shows the polar motion coordinates for the CIP; note the defined direction of y, which is opposite to the y-axis of the right-handed system of Fig. 2.7. Viewed as horizontal Cartesian coordinates, their values change by only a few meters over several years; typically they are given by the subtended central angle, where 1″ corresponds approximately to 30 m on the Earth's surface.

The principal component of polar motion is the *Chandler wobble*. This is basically the free Eulerian motion which would have a period of about 304 days, based on the moments of inertia of the Earth, if the Earth were a rigid body. Due to the elastic yielding of the Earth, resulting in displacements of the maximum

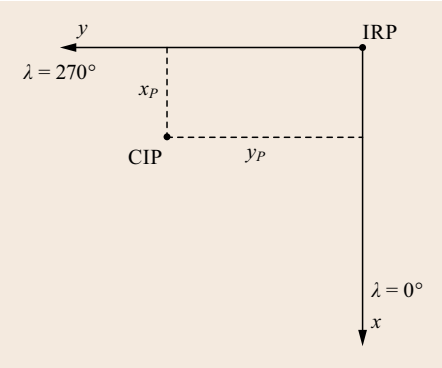

Fig. 2.23 Polar motion coordinates

moment of inertia, this motion has a longer period of about 430 days. S. C. Chandler observed and analyzed this discrepancy in the period in 1891; and, Newcomb gave the dynamical explanation [2.79, p. 80], thus also proving that the Earth is, in fact, not a rigid body. The period of this main component of polar motion is called the *Chandler* period; its amplitude is about 0.2 arcsec. Other components of polar motion include the approximately annual signal due to the redistribution of masses by way of meteorological and geophysical processes, with an amplitude of about 0.05–0.1″, and the *nearly diurnal free wobble*, due to the slight misalignments of the rotation axes of the mantle and liquid outer core (also known as the *free core nutation*, with magnitude of about $0.1–0.3 \cdot 10^{-3}$″ and period of about 430 days with respect to the celestial sphere). Finally, there is the so-called *polar wander*, which is the secular motion of the pole. During 1900–2000, Earth's spin axis wandered about 0.004″ per year in the direction of the 280° meridian. Figure 2.24 shows the polar motion for the period 2000–2010, and also the general drift for the last 110 years.

If $\boldsymbol{r}_e$ is a unit vector that defines a geocentric direction of a point in the terrestrial reference system in terms of spherical coordinates

$$\boldsymbol{r}_e = \begin{pmatrix} \cos\lambda\cos\phi \\ \sin\lambda\cos\phi \\ \sin\phi \end{pmatrix} , \tag{2.67}$$

then the transformation from the terrestrial reference pole to the instantaneous, or intermediate pole (CIP), is given with appropriate rotations by

$$\begin{aligned} \boldsymbol{r}_i &= \mathbf{R}_1(y_\mathrm{p})\mathbf{R}_2(x_\mathrm{p})\,\boldsymbol{r}_e \\ &= \mathbf{W}\,\boldsymbol{r}_e \end{aligned} \tag{2.68}$$

Just as the instantaneous celestial system has a nonrotating origin for right ascension, one may define an

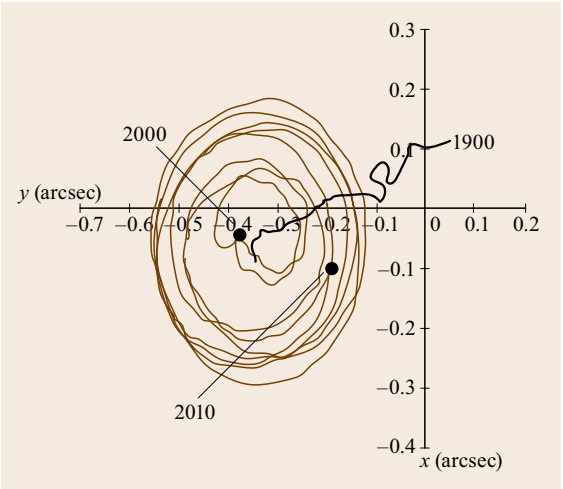

Fig. 2.24 Polar motion from 2000 to 2010, and polar wander since 1900. Polar motion coordinates are obtained from IERS and are smoothed to obtain the trend

instantaneous terrestrial system that has a nonrotating origin for longitudes, called the *Terrestrial Intermediate Origin* (TIO). In this way, the only difference between the instantaneous celestial and terrestrial systems is Earth's rotation; the polar axes are the same.

With a derivation completely analogous to that for the precession–nutation matrix, $\mathbf{Q}$, the polar motion matrix is

$$\begin{aligned} \mathbf{W} &= \mathbf{R}_3(-s') \\ &\quad \times \begin{pmatrix} 1-a'x_\mathrm{p}^2 & a'x_\mathrm{p}y_\mathrm{p} & -x_\mathrm{p} \\ a'x_\mathrm{p}y_\mathrm{p} & 1-a'y_\mathrm{p}^2 & y_\mathrm{p} \\ x_\mathrm{p} & -y_\mathrm{p} & 1-a'(x_\mathrm{p}^2+y_\mathrm{p}^2) \end{pmatrix} , \end{aligned} \tag{2.69}$$

where $a' = 1/2 + \left(x_\mathrm{p}^2 + y_\mathrm{p}^2\right)/8$. The parameter s' defines the location of the TIO on the instantaneous equator through an expression that is analogous to (2.66). By neglecting terms of second and higher orders, the exact equation (2.69) is approximately equal to

$$\mathbf{W} = \mathbf{R}_3(-s')\mathbf{R}_1(y_\mathrm{p})\mathbf{R}_2(x_\mathrm{p}) . \tag{2.70}$$

Furthermore, s' is significant only because of the largest components of polar motion and an approximate model is given by

$$s' = -0.0015'' \left(\frac{a_c^2}{1.2} + a_a^2\right)\tau , \tag{2.71}$$

where a_c and a_a are the amplitudes, in arcsec, of the Chandler wobble ($\mathcal{O}(0.2'')$) and the annual wobble

($\mathcal{O}(0.05'')$). Hence, the magnitude of s' is of the order of $0.1 \cdot 10^{-3}$ arcsec.

The polar motion coordinates are tabulated by the IERS as part of the Earth Orientation Parameters (EOP) and predicted on the basis of observations, such as from VLBI and satellite ranging. Thus, **W** is a function of time, but there are no analytic models for polar motion as there are for precession and nutation. For the highest precision, the polar motion coordinates should be amended to include motions corresponding to nutations and tidal effects [2.6, Chaps. 5 and 8] with periods less than 2 days in the GCRS in order to comply with the definition of the intermediate pole.

2.5.4 Transformations

It is the current convention to formulate the transformation between celestial and terrestrial reference systems via an intermediate system. This intermediate, or true, or epoch-of-date system describes either precession and nutation when transformed from the celestial reference system, or polar motion and Earth rotation when transformed from the terrestrial reference system. As a dynamical system it is not a reference system since coordinates in this system vary significantly in time. For this reason, the intermediate system has also been called an *ephemeris* system. The newer *intermediate* nomenclature, more descriptive of the system's function, was adopted through a number of resolutions by the IAU during 2000–2006.

The ideal choice of the intermediate system largely falls on the choice of polar axis since the choice for the origin of the intermediate right ascension is now fixed by the nonrotating origin. In 1979 this pole was defined as having no motions with periods less than 2 days either with respect to the celestial or the terrestrial reference systems. The 2-day restriction on periods was consistent with the observational capability at the time to resolve such motions. The *Celestial Ephemeris Pole* (CEP), thus defined, divided the observable polar motion and predictable precession/nutations.

With improved VLBI observational techniques and data processing, shorter periods of motion could be discerned and in 2000 the IAU resolved to refine the definition of the intermediate pole. The newly named *celestial intermediate pole* (CIP) by definition, like the CEP, moves on the celestial sphere with periods greater than 2 days (frequencies less than ± 0.5 cycles per sidereal day, cpsd). This includes all the conventional predictable precessions and nutations produced by external gravitational torques on the Earth. Also included are the observed polar motions within $\pm$ 0.5 cpsd of Earth's diurnal rotation frequency (the *diurnal retrograde band*) since it can be shown that they are equivalent to nutations with periods larger than 2 days. The terrestrial motions of the CIP, on the other hand, are defined to be those with frequencies outside the diurnal retrograde band. They not only include the conventional polar motions, such as the Chandler wobble, but also the high-frequency nutations, which are equivalent to polar motions outside this band. For additional details on these conventions, see [2.78, 88] and [2.75, p. 86].

It has been argued [2.89] that the intermediate pole is not essential in the transformation between the terrestrial and the celestial frame and that a combination of model and observations in a single transformation avoids much confusion and debate about the definition of the CIP. However, with current conventions the practical transformation between celestial and terrestrial reference frames combines the transformations (2.58) and (2.68) with Earth rotation,

$$\boldsymbol{r}_{\mathrm{TRS}} = \mathbf{W}^{\top}\mathbf{R}_3(\theta)\mathbf{Q}^{\top}\boldsymbol{r}_{\mathrm{CRS}} \,, \tag{2.72}$$

where θ is the Earth rotation angle (Sect. 2.1.3). This is called the *CIO method* of transformation, referring to the new convention of defining the origin for right ascension in the intermediate celestial system by the nonrotating origin. Alternatively, the so-called *equinox method*, uses the Greenwich sidereal time for the angle of Earth's rotation and the traditional precession and nutation series, given by (2.56)

$$\boldsymbol{r}_{\mathrm{TRS}} = \mathbf{W}^{\top}\mathbf{R}_3(\mathrm{GAST})\mathbf{NPB}\,\boldsymbol{r}_{\mathrm{CRS}} \,. \tag{2.73}$$

where a small rotation, **B**, is included to account for the frame bias.

Equations (2.72) and (2.73), of course, can be reversed to obtain coordinates in the CRF from coordinates in the terrestrial reference frame by noting that each rotation matrix is orthogonal – its inverse is its transpose

$$\boldsymbol{r}_{\mathrm{CRS}} = \mathbf{Q}\mathbf{R}_3^{\top}(\theta)\mathbf{W}\boldsymbol{r}_{\mathrm{TRS}} \tag{2.74}$$

and

$$\boldsymbol{r}_{\mathrm{CRS}} = \mathbf{B}^{\top}\mathbf{P}^{\top}\mathbf{N}^{\top}\mathbf{R}_3^{\top}(\mathrm{GAST})\mathbf{W}\boldsymbol{r}_{\mathrm{TRS}} \,. \tag{2.75}$$

In applying the transformation (2.72), or (2.73), to observed points on the celestial sphere, it is important to consider any observational effects on the celestial coordinates of objects, such as actual, or proper motion (e.g., of stars), parallax due to the observer's changing position relative to the barycenter, and aberration due to the velocity of the observer relative to the barycenter. These effects are of primary interest for directional (e.g., optical or VLBI) observations of celestial bodies

but of limited relevance for GNSS data processing. For a detailed description, interested readers are referred to [2.5].

No matter whether the *equinox method* or the *CIO method* is adopted, the CRF-to-TRF transformation is characterized by extremely lengthy series expansions of the respective rotation angles. In order to facilitate the correct and consistent application of the conventional transformation, all relevant coefficients are made available in electronic form [2.84] by the IERS. Furthermore, various computer implementations of the transformations (or selected aspects thereof) are offered by the IAU, the IERS, and individual authors. Such software may be applied directly, as a reference for validating independent implementations, or simply for better understanding of the underlying transformation concepts. Common examples include, for example, the IAU Standards of Fundamental Astronomy (SOFA, [2.90]) and the AstroRef package of [2.74]. Computational and implementation issues of the transformations are addressed in [2.91, 92]. Among others, the authors highlight the benefit of interpolating from a grid of precomputed values, when evaluating the transformation for a dense set of nearby epoch values.

2.6 Perspectives

This chapter has introduced the basic concepts of modern space–time reference systems and frames that have jointly been developed by astronomers and geodesists as a basis of their work. They enable a concise description of the Earth's motion in space and the location of objects on or near the Earth. Users of global navigation satellite systems are inevitably confronted with the issue of coordinates and reference systems, when it comes to the exchange and proper understanding of measured positions. Since GNSS provides essentially four-dimensional observations, with time as the fourth component of the navigation solution, the underlying concepts and conventions of time measurements are therefore equally important in all aspects of GNSS navigation.

Different GNSSs such as GPS, GLONASS, BeiDou, and Galileo have historically employed different time frames (realized by independent atomic clocks) and spatial reference frames (realized by different fundamental reference stations and partly different techniques). This affects the satellite orbit and clock information provided to the users and impacts a consistent navigation solution based on observations of multiple GNSS constellations. Fortunately, much progress has been achieved over the past decade. Individual frame realizations as used by the various GNSSs today exhibit centimeter-level differences that are well below the typical meter level accuracy of broadcast navigation information. Still, however, systematic time offsets (at the 10–100 ns level) between GNSS-specific time scales need to be carefully considered in the positioning and taken into account in the employed algorithms (Chap. 21).

Considering the high-level of accuracy that can today be achieved through carrier-phase-based GNSS positioning techniques, users are confronted with the fact that the Earth's crust is far from solid and itself subject to permanent changes. This includes both long-term changes such as tectonic plate motion (Sect. 2.3.2) but also periodic site shifts due to solid Earth and ocean tides (Sect. 2.3.5). Even though differential GNSS positioning techniques (Chap. 26) can offer (relative) accuracies down to the millimeter level, their use is largely unaffected by such intricate details. Undifferenced, precise point positioning (PPP) techniques, in contrast, aim at providing absolute positions in a global reference frame. Here, a proper understanding of the underlying frame definitions and the consistent application of conventional corrections (e.g., for frame motion or tides) in the PPP software becomes an essential aspect of the GNSS data processing (Chap. 25). Similarity transformations between different regional and global frames (Sect. 2.3.4) or the transition between ellipsoidal and geoid heights (Sect. 2.3.1) are likewise important aspects of GNSS surveying (Chap. 35) and geodesy (Chap. 36).

While most precise GNSS users can confine themselves to a proper understanding of terrestrial reference systems and frames, the relation betwen celestial and terrestrial frames as discussed in Sect. 2.5 is likewise of relevance for various specific aspects of GNSS data processing. This includes, for example, the generation of GNSS precise orbit products (Chap. 34) and the GNSS-based precise orbit determination of satellites in low Earth orbit (Chap. 32). Satellite orbits and their equations of motion are most naturally expressed in a celestial frame, while the locations of GNSS monitoring stations are best described in a terrestrial frame. Conventional relations for the CRF-to-TRF transformation are essential for consistency of products obtained by individual analysis centers. On the other hand, the joint adjustment of satellite orbits, site locations, and Earth orientation parameters has become a vital part of space geodesy (Chap. 36) and contributes to a continued improvement of references frames and the understanding of Earth rotation.

References

2.1 D.D. McCarthy, K.P. Seidelmann: *Time: From Earth Rotation to Atomic Physics* (Wiley-VCH, Weinheim 2009)

2.2 K. Lambeck: *Geophysical Geodesy, The Slow Deformations of the Earth* (Clarendon, Oxford 1988)

2.3 B.N. Taylor, A. Thompson (Eds.): *The International System of Units (SI)*, NIST SP 330 (National Institute of Standards and Technology, Gaithersburg 2008)

2.4 SI Brochure: The International System of Units (SI), 8th edn. (Bureau International des Poids et Mesures, Paris 2006)

2.5 P.K. Seidelmann: *Explanatory Supplement to the Astronomical Almanac* (Univ. Science Books, Mill Valley 1992)

2.6 G. Petit, B. Luzum: *IERS Conventions*, IERS Technical Note No. 36 (Verlag des Bundesamts für Kartographie und Geodäsie, Frankfurt 2010)

2.7 C. Audoin, B. Guinot: *The Measurement of Time: Time, Frequency and the Atomic Clock* (Cambridge Univ. Press, Cambridge 2001)

2.8 Bureau International des Poids et Mesures: BIPM Circular T, ftp://ftp2.bipm.org/pub/tai/publication/cirt

2.9 SI Brochure: Practical realization of the definition of the unit of time. In: *The International System of Units (SI)*, 8th edn. (Bureau International des Poids et Mesures, Paris, 2006) App. 2

2.10 D.D. McCarthy: Using UTC to determine the Earth's rotation angle, Proc. Coll. Explor. Implic. Redefining Coord. Univers. Time (UTC), Exton, ed. by S.L. Allen, J.H. Seago, R.L. Seaman (Univelt, San Diego 2011) pp. 105–116

2.11 Standard-Frequency and Time-Signal Emissions, ITU-R Recommendation TF.460-6 (International Telecommunication Union, Radio-communication Bureau, Geneva, Feb. 2002)

2.12 USNO: TAI minus UTC time difference ftp://maia.usno.navy.mil/ser7/tai-utc.dat

2.13 R.A. Nelson, D.D. McCarthy: S.N. Malys, J. Levine, B. Guinot, H. F. Fliegel, R. L. Beard, T. R. Bartholomew: The leap second: its history and possible future, Metrologia **38**(6), 509 (2001)

2.14 D. Finkleman, J.H. Seago, P.K. Seidelmann: The debate over UTC and leap seconds, Proc. AIAA Guid. Navig. Control Conf. Toronto (AIAA, Reston 2010), AAIA 2010–8391

2.15 P.K. Seidelmann, J.H. Seago: Time scales, their users, and leap seconds, Metrologia **48**(4), S186–S194 (2011)

2.16 W. Lewandowski, E.F. Arias: GNSS Times and UTC, Metrologia **48**(4), S219–S224 (2011)

2.17 K.R. Brown Jr.: The theory of the GPS composite clock, Proc. ION GPS 91, Albuquerque (ION, Virginia 1991) pp. 223–241

2.18 A.L. Satin, W.A. Feess, H.F. Fliegel, C.H. Yinger: GPS composite clock software performance, Proc. 22rd Annu. PTTI Meet. Vienna (JPL, Pasadena 1991) pp. 529–546

2.19 H.S. Mobbs, S.T. Hutsell: Refining monitor station weighting in the GPS composite clock, Proc. 29th Annu. PTTI Meet. Long Beach (JPL, Pasadena 1997)

2.20 Navstar GPS Space Segment/Navigation User Segment Interfaces, Interface Specification, IS-GPS-200H, 24 Sep. 2013 (Global Positioning Systems Directorate, Los Angeles Air Force Base, El Segundo 2013)

2.21 T.E. Parker, D. Matsakis: Time and frequency dissemination: Advances in GPS transfer techniques, GPS World **15**(11), 32–38 (2004)

2.22 Global Navigation Satellite System GLONASS – Interface Control Document, v5.1, (Russian Institute of Space Device Engineering, Moscow 2008)

2.23 P. Zhang, C. Xu, C. Hu, Y. Chen, J. Zhao: Time scales and time transformations among satellite navigation systems, Proc. CSNC 2012, Guanzhou, Vol. II, ed. by J. Sun, J. Liu, Y. Yang, S. Fan (Springer, Berlin 2012) pp. 491–502

2.24 A.V. Druzhin, V. Palchikov: Current state and perspectives of UTC(SU) broadcast by GLONASS, 9th Meet. Int. Comm. GNSS (ICG), Prague (UNOOSA, Vienna 2014) pp. 1–9

2.25 R. Zanello, M. Mascarello, L. Galleani, P. Tavella, E. Detoma, A. Bellotti: The Galileo precise timing facility, Proc. IEEE FCS 2007 21st EFTF, Geneva (2007) pp. 458–462

2.26 X. Stehlin, Q. Wang, F. Jeanneret, P. Rochat, E. Detoma: Galileo system time physical generation, Proc. 38th Annu. PTTI Meet. Washington, DC (JPL, Pasadena 2006) pp. 395–406

2.27 C. Han, Y. Yang, Z. Cai: BeiDou navigation satellite system and its time scales, Metrologia **48**(4), S213–S218 (2011)

2.28 R. Hlaváč, M. Lösch, F. Luongo, J. Hahn: Timing infrastructure for Galileo system, Proc. 20th EFTF, Braunschweig (2006) pp. 391–398

2.29 BeiDou Navigation Satellite System Signal In Space Interface Control Document – Open Service Signal, Version 2.0 (China Satellite Navigation Office, 2013)

2.30 W. Torge, J. Müller: *Geodesy* (Walter de Gruyter, Berlin 2012)

2.31 K.M. Borkowski: Accurate algorithms to transform geocentric to geodetic coordinates, Bull. Géodésique **63**(1), 50–56 (1989)

2.32 D.D. McCarthy: *IERS Conventions (1996)*, IERS Technical Note No. 21 (Observatoire de Paris, Paris 1996)

2.33 T. Fukushima: Transformation from Cartesian to geodetic coordinates accelerated by Halley's method, J. Geod. **79**(12), 689–693 (2006)

2.34 H. Moritz: Geodetic reference system 1980, Bull. Géodésique **54**(3), 395–405 (1980)

2.35 E. Groten: Fundamental arameters and current (2004) best estimates of the parameters of common relevance to astronomy, geodesy, and geodynamics, J. Geod. **77**, 724–731 (2004)

2.36 J. Kovalevsky, I.I. Mueller: Comments on conventional terrestrial and quasi-inertial reference systems. In: *Reference Coordinate Systems for Earth Dynamics*, ed. by E.M. Gaposchkin, B. Kołczek (D. Reidel, Dordrecht 1981) pp. 375–384

2.37 H. Moritz, I.I. Mueller: *Earth Rotation: Theory and Observation* (Unger, New York 1987)

2.38 Geodetic Glossary (National Geodetic Survey, National Oceanic and Atmospheric Administration, Rockville 1986)
2.39 G. Seeber: *Satellite Geodesy: Foundations, Methods, and Applications* (Walter de Gruyter, Berlin 2003)
2.40 H. Schuh, D. Behrend: VLBI: A fascinating technique for geodesy and astrometry, J. Geodyn. **61**, 68–80 (2012)
2.41 R.A. Snay, T. Soler: Continuously operating reference station (CORS): History, applications, and future enhancements, J. Surv. Eng. **134**(4), 95–104 (2008)
2.42 B. Hofmann-Wellenhof, H. Moritz: *Physical Geodesy* (Springer, Berlin 2005)
2.43 N.K. Pavlis, S.A. Holmes, S.C. Kenyon, J.K. Factor: The development and evaluation of the Earth Gravitational Model 2008 (EGM2008), J. Geophys. Res. Solid Earth **117**(B4), 2156–2202 (2012)
2.44 Standardization Agreement Navstar Global Positioning System (GPS) System Characteristics, STANAG 4294, 1st edn. (North Atlantic Treaty Organization, 1993)
2.45 S. Malys, J.H. Seago, N.K. Pavlis, P.K. Seidelmann, G.H. Kaplan: Why the Greenwich meridian moved, J. Geod. **89**(12), 1263–1272 (2015)
2.46 Z. Altamimi, X. Collilieux, L. Métivier: ITRF2008: An improved solution of the International Terrestrial Reference Frame, J. Geod. **85**(8), 457–473 (2011)
2.47 M.R. Pearlman, J.J. Degnan, J.M. Bosworth: The international laser ranging service, Adv. Space Res. **30**(2), 135–143 (2002)
2.48 L. Combrinck: Satellite laser ranging. In: *Sciences of Geodesy*, Vol. I, ed. by G. Xu (Springer, Berlin 2010) pp. 301–338
2.49 M. Meindl, G. Beutler, D. Thaller, R. Dach, A. Jäggi: Geocenter coordinates estimated from GNSS data as viewed by perturbation theory, Adv. Space Res. **51**(7), 1047–1064 (2013)
2.50 S.P. Kuzin, S.K. Tatevian, S.G. Valeev, V.A. Fashutdinova: Studies of the geocenter motion using 16-years DORIS data, Adv. Space Res. **46**(10), 1292–1298 (2010)
2.51 Z. Altamimi, C. Boucher, P. Sillard: New trends for the realization of the international terrestrial reference system, Adv. Space Res. **30**(2), 175–184 (2002)
2.52 Z. Altamimi, P. Sillard, C. Boucher: ITRF2000: A new release of the International Terrestrial Reference Frame for Earth science applications, J. Geophys. Res. **107**(B10), 2214 (2002)
2.53 D.F. Argus, R.G. Gordon: No-net-rotation model of current plate velocities incorporating plate motion model NUVEL-1, Geophys. Res. Lett. **18**(11), 2039–2042 (1991)
2.54 C. DeMets, R.G. Gordon, D.F. Argus, S. Stein: Effect of recent revisions to the geomagnetic reversal time scale on estimates of current plate motions, Geophys. Res. Lett. **21**(20), 2191–2194 (1994)
2.55 Z. Altamimi, L. Métivier, X. Collilieux: ITRF2008 plate motion model, J. Geophys. Res. **117**(B07402), 1–14 (2012)
2.56 Department of Defense World Geodetic System 1984 (WGS84): Its definition and relationships with local geodetic systems, Publication NIMA TR8350.2, 3rd edn., amendm. 1 (National Imagery and Mapping Agency, 2000)
2.57 Supplement to Department of Defense World Geodetic System 1984 Technical Report, Part I, DMA TR 8350.2-A (Defense Mapping Agency, Washington 1987)
2.58 M.J. Merrigan, E.R. Swift, R.F. Wong, J.T. Saffel: A refinement to the World Geodetic System 1984 reference frame, Proc. ION GPS 2002, Portland (IOM, Virginia 2002) pp. 1519–1529
2.59 R.F. Wong, C.M. Rollins, C.F. Minter: Recent Updates to the WGS 84 Reference Frame, Proc. ION GNSS 2012, Nashv. (ION, Virginia 2012) pp. 1164–1172
2.60 S.G. Revnivykh: GLONASS status and progress, 47th CGSIC Meet. Fort Worth (2007)
2.61 Parametry Zemli 1990 (PZ-90.11) Reference document (Military Topographic Department of the General Staff of Armed Forces of the Russian Federation, Moscow 2014)
2.62 A.N. Zueva, E.V. Novikov, D.I. Pleshakov, I.V. Gusev: System of geodetic parameters "Parametry Zemli 1990" PZ-90.11, 9th Meet. Int. Comm. GNSS (ICG), Work. Group D, Prague (UNOOSA, Vienna 2014)
2.63 Y. Yang: Chinese Geodetic Coordinate System 2000, Chin. Sci. Bull. **54**(15), 2714–2721 (2009)
2.64 G. Gendt, Z. Altamimi, R. Dach, W. Söhne, T. Springer, GGSP Prototype Team: GGSP: Realisation and maintenance of the Galileo terrestrial reference frame, Adv. Space Res. **47**(2), 174–185 (2011)
2.65 D. D. McCarthy: *IERS Conventions (1992)*, IERS Technical Note No. 13 (Observatoire de Paris, Paris 1992)
2.66 International Terrestrial Reference Frame: ITRF Transformation Parameters, ITRF Website http://itrf.ensg.ign.fr/trans_para.php
2.67 T. Soler, R.A. Snay: Transforming positions and velocities between the International Terrestrial Reference Frame of 2000 and North American Datum of 1983, J. Surv. Eng. **130**(2), 49–55 (2004)
2.68 IAG: IAG resolutions adopted at the XXth IUGG General Assembly in Vienna, Bulletin Géodésique **66**(2), 132–133 (1992)
2.69 M. Poutanen, M. Vermeer, J. Mäkinen: The permanent tide in GPS positioning, J. Geod. **70**(8), 499–504 (1996)
2.70 P.M. Mathews, B.A. Buffett, I.I. Shapiro: Love numbers for a rotating spheroidal Earth: New definitions and numerical values, Geophys. Res. Lett. **22**(5), 579–582 (1995)
2.71 J.M. Wahr: Deformation induced by polar motion, J. Geophys. Res. Solid Earth **90**(B11), 9363–9368 (1985)
2.72 P.M. Mathews, B.A. Buffett, I.I. Shapiro: Love numbers for diurnal tides: Relation to wobble admittances and resonance expansions, J. Geophys. Res. **100**(B6), 9935–9948 (1995)
2.73 W.E. Farrell: Deformation of the Earth by surface loads, Rev. Geophys. **10**(3), 761–797 (1972)
2.74 M. Soffel, R. Langhans: *Space-Time Reference Systems* (Springer, Berlin 2012)
2.75 V. Dehant, P.M. Mathews: *Precession, Nutation and Wobble of the Earth* (Cambridge Univ. Press, Cambridge 2015)

2.76 E.W. Woolard: *Theory of the Rotation of the Earth Around its Center of Mass*, Astronomical Papers Vol. XV Part 1 (U.S. Naval Observatory, Washington, D.C. 1953)

2.77 J.H. Lieske, T. Lederle, W. Fricke, B. Morando: Expressions for the precession quantities based upon the IAU/1976/system of astronomical constants, Astron. Astrophys. **58**, 1–16 (1977)

2.78 N. Capitaine, P.T. Wallace, J. Chapront: Expressions for IAU 2000 precession quantities, Astron. & Astrophys. **412**(2), 567–586 (2003)

2.79 I.I. Mueller: *Spherical and Practical Astronomy as Applied to Geodesy* (F. Ungar, New York 1969)

2.80 H. Goldstein, C.P. Poole, J.L. Safko: *Classical Mechanics* (Addison Wesley, San Francisco 2000)

2.81 N. Capitaine, P.T. Wallace, J. Chapront: Improvement of the IAU 2000 precession model, Astron. & Astrophys. **432**(1), 355–367 (2005)

2.82 J.P. Vinti: *Orbital and Celestial Mechanics* (AIAA, Reston 1998)

2.83 H. Kinoshita: Theory of the rotation of the rigid Earth, Celest. Mech. **15**(3), 277–326 (1977)

2.84 International Earth Rotation and Reference Systems Service: IERS Conventions 2010, electronic supplement http://62.161.69.134/iers/conv2010/conv2010_c5.html

2.85 N. Capitaine, B. Guinot, J. Souchay: A non-rotating origin on the instantaneous equator: Definition, properties and use, Celest. Mech. **39**(3), 283–307 (1986)

2.86 N. Capitaine: The celestial pole coordinates, Celest. Mech. Dyn. Astron. **48**(2), 127–143 (1990)

2.87 D.D. McCarthy, G. Petit: *IERS Conventions (2003)*, IERS Technical Note No. 36 (Verlag des Bundesamts für Kartographie und Geodäsie, Frankfurt 2004)

2.88 P.M. Mathews, P. Bretagnon: Polar motions equivalent to high frequency nutations for a nonrigid Earth with anelastic mantle, Astron. & Astrophys. **400**(3), 1113–1128 (2003)

2.89 P. Mathews, T. Herring: On the reference pole for Earth orientation and UT1, Proc. IAU Colloq. 180: Towards Models Constants Sub-Microarcsecond Astrom. Washington DC, ed. by K.J. Johnston, D.D. McCarthy, B.J. Luzum, G.H. Kaplan (US Naval Observatory, Washington, DC 2000) pp. 164–170

2.90 IAU SOFA Board: IAU SOFA Software Collection (International Astronomical Union), IAU SOFA Center http://www.iausofa.org

2.91 D.A. Vallado, J.H. Seago, P.K. Seidelmann: Implementation issues surrounding the new IAU reference systems for astrodynamics, Proc. 16th AAS/AIAA Space Flight Mech. Conf. Tampa (AAS, San Diego 2006), pp. 1–22, AAS 06-134

2.92 V. Coppola, J.H. Seago, D.A. Vallado: The IAU 2000A and IAU 2006 precession-nutation theories and their implementation, Proc. 19th AAS/AIAA Space Flight Mech. Meet. Savannah (AAS, San Diego 2009), pp. 1–20, AAS 09-159